Causes of climate change over the historical record

Causes of climate change over the historical record

Causes of climate change over the entire industrial era

Gabriele C Hegerl[1]; Stefan Brönnimann[2], Tim Cowan[3]; Andrew R Friedman[1]; Ed Hawkins[4]; Carley Iles[5]; Wolfgang Müller[6]; Andrew Schurer[1], Sabine Undorf[1]

1: School of Geosciences, University of Edinburgh, Edinburgh, UK

2: Oeschger Centre for Climate Change Research and Institute of Geography, University of Bern, Bern Switzerland

3: University of Southern Queensland & Bureau of Meteorology, Melbourne, Australia

4: National Centre for Atmospheric Science, Department of Meteorology, University of Reading, Reading, UK

5: Laboratoire des Sciences du Climat et de l'Environnement, LSCE/IPSL, CEA-CNRS-UVSQ, Université Paris-Saclay, F-91198 Gif-sur-Yvette, France

6: Max-Planck Institute for Meteorology, Hamburg, Germany

Abstract

This review addresses the causes of observed climate variations across the industrial period, from 1750 to present. It focuses on long-term changes, both in response to external forcing and to climate variability in the ocean and atmosphere. A synthesis of results from attribution studies based on palaeoclimatic reconstructions covering the recent few centuries to the 20th century, and instrumental data shows how greenhouse gases began to cause warming since the beginning of industrialization, causing trends that are attributable to greenhouse gases by 1900 in proxy-based temperature reconstructions. Their influence increased over time, dominating recent trends. However, other forcings have caused substantial deviations from this emerging greenhouse warming trend: volcanic eruptions have caused strong cooling following a period of unusually heavy activity, such as in the early 19th century; or warming during periods of low activity, such as in the early-to-mid 20th century. Anthropogenic aerosol forcing most likely masked some global greenhouse warming over the 20th century, especially since the accelerated increase in sulphate aerosol emissions starting around 1950. Based on modelling and attribution studies, aerosol forcing has also influenced regional temperatures, caused long-term changes in monsoons and imprinted on Atlantic variability. Multi-decadal variations in atmospheric modes can also cause long-term climate variability, as apparent for the example of the North Atlantic Oscillation, and have influenced Atlantic ocean variability. Long-term precipitation changes are more difficult to attribute to external forcing due to spatial sparseness of data and noisiness of precipitation changes, but the observed pattern of precipitation response to warming from station data supports climate model simulated changes and with it, predictions. The long-term warming has also led to significant differences in daily variability as, for example, visible in long European station data. Extreme events over the historical record provide valuable samples of possible extreme events and their mechanisms.

1. Introduction

Much of the research on climate change and climate variability has been on analyses focusing on the second half of the 20th century. This is highlighted by the conclusion of the 5th Assessment Report (AR5) of the Intergovernmental Panel on Climate Change (IPCC) that "it is extremely likely that more than half of the observed increase in global average surface temperature from 1951 to 2010 was

caused by the anthropogenic increase in greenhouse gas concentrations and other anthropogenic forcings together" (Bindoff et al., 2014). That statement was supported by analyses using the full instrumental time horizon, but results are clearer and uncertainties better understood when focusing on the past 60 years (see e.g. Jones et al., 2013; Gillett et al., 2012). However, some analyses focus on the entire historical record or a large fraction of it, starting with Andronova and Schlesinger (2000) and Hulme and Jones, 1994), and multiple analyses of the instrumental period are available. The IPCC report on 1.5 degrees of warming concluded, based on multiple attribution analyses, that 'Estimated anthropogenic global warming matches the level of observed warming to within ±20% (likely range)' (IPCC, 2018).

Much of the analysis of extreme events also focuses on recent events, including attributing causes to extreme events soon after they occurred (Stott et al., 2016; Stott et al., 2018), but the historical and early instrumental record contains a wealth of information on past events that if used with caution can provide valuable samples of possible events. Also, while decadal prediction tools are tested on hindcasts of the recent past, some analyses suggest decadal changes in predictability and hence biased results when limiting hindcasts to only a few decades (O'Reilly et al., 2017; Weisheimer et al., 2017), again emphasising the benefit of using the full record.

Focusing on the recent past has clear advantages: Observational data are much more complete and reliable, particularly over the satellite period when global or near-global coverage emerged. In contrast, early instrumental data show increasing gaps further back in time (Morice et al., 2012), and are affected by uncertainty due to changing sea surface temperature (SST) measurement practices (Kennedy et al., 2011a, 2011b; Kent et al., 2016; Morice et al., 2012; Thompson et al., 2008). However, a longer time horizon better constrains the response to forcing (Gillett et al., 2012; Jones et al., 2013), and reduces spurious correlation between forcings that can yield degenerate results. A longer time horizon also provides a better sample of internal climate variability, particularly of decadal modes. This is important as a short sample can make it harder to tease apart the contribution of variability generated within the climate system and that occurring in response to forcing, for example, in the case of the Atlantic Multidecadal Variability (AMV; e.g., Booth et al., 2012; Knight, 2009; Tandon and Kushner, 2015; Ting et al., 2009; Undorf et al., 2018a). Lastly, analyses of the instrumental period and the last millennium overlap, with some long instrumental records stretching back into the 17th century (Manley, 1974; Rousseau, 2015). Estimates of global temperature based on palaeoclimatic data are spatially sparse, but more evenly spaced across the globe (e.g., Crowley et al., 2014). Some regional reconstructions successfully use a combination of long historical records with proxy information (Luterbacher et al., 2004), yet the most recent results attributing fluctuations to external forcing are based on analysis of either instrumental data or proxy-based reconstructions (e.g., PAGES 2k Consortium et al., 2013), and the results have not been brought together in a coherent framework.

Here we discuss causes of climate change and estimates of climate variability over a longer time horizon, stretching over the length of the instrumental global data into the 19th century; and linking results to those from analyses of the last millennium. For precipitation, we focus on changes over the 20th century due to the sparsity of earlier records and the need for better sampling to record spatially inhomogeneous changes. We also discuss the contribution to multidecadal trends by variability generated within the climate system, both in the atmosphere and ocean. For the latter topic we focus on the Atlantic Sector due to better coverage back in time. Specifically, we address the following questions:

- When did the response to greenhouse gases emerge on hemispheric and global scales?

- What factors cause decadal and multidecadal deviations from the greenhouse warming trend?
- How can analysis of data prior to 1950 contribute to understanding and quantifying climate change?

The paper briefly discusses methods and data, followed by a review of causes of climate change over the industrial period (Section 3), a brief review of causes and consequences of multidecadal climate variability (Section 4), and of related extremes (Section 5) and draws some conclusions and recommendations.

2. Data and Methods

Data sources become sparser and their quality worse back in time, with observations largely limited to the surface of the Earth. Gridded global instrumental surface temperature data sets (Jones et al., 2012; Morice et al., 2012) presently stretch to 1850, with estimates of uncertainty available that include both the effect of sampling uncertainty and systematic changes in measurement techniques, such as different types of buckets (Folland and Parker, 1995). While the record is fairly well researched, issues continue to be discovered, such as an inhomogeneity in SST data in the 1940s (Thompson et al., 2008); and ongoing offsets due to differences in observing fleets (Chan and Huybers, 2019). Long, homogenized instrumental surface temperature records go back to the 18th century for some European locations such as Milan, Stockholm, and Central England, resolving daily variability (e.g., Maugeri et al., 2002; Moberg et al., 2002; Parker et al., 1992), while the US Global Historical Climatology Network dataset also contains a limited number of long daily recordings (see e.g., Kenyon and Hegerl, 2008). Homogeneity can be an issue for long stations. For example, there is a hot bias for sunny days due to the lack of shielding of summer temperature measurements before the invention of the Stevenson screen in 1864 (Böhm et al., 2010; Naylor, 2019; Stevenson, 1864). There is considerable scope to extend the instrumental record back in time, using long stations and undigitized records (e.g., Brönnimann et al. 2019b).

Long-term gridded precipitation datasets (Becker et al., 2013; Harris et al., 2014; Zhang et al., 2007) are sparse, particularly prior to the middle of the 20th century. Reconstructions are available for past hemispheric and continental-scale temperature and to a lesser extent also for drought (e.g., Anchukaitis et al., 2017; Luterbacher et al., 2004; PAGES 2k Consortium et al., 2013; Steiger et al., 2018). Also, sea ice data from the early 20th century are being increasingly digitised, allowing better reflection, for example, of the early 20th century sea ice retreat in data (Titchner and Rayner, 2014; Walsh et al., 2017; Hegerl et al., 2018).

Global coverage of the 3-D atmosphere is available from historical reanalyses that assimilate surface and sea level pressure and, in some products, marine winds (Compo et al., 2011; Laloyaux et al., 2018; Poli et al., 2016). These provide a dynamically consistent estimate of the atmospheric state from 1871–2008, with updates in preparation going back further. Changes in data support can introduce inhomogeneities in reanalyses over time, hence trends have to be treated with caution (e.g., Ferguson and Villarini, 2012; Krüger et al., 2012). Inhomogeneities are less of a concern where analysis is constrained to the response to well observed modes of climate variability or to episodic forcing such as volcanic eruptions. Hence, with caution, the reanalyses can inform on causes and dynamical links of past anomalies. Reanalyses are now being pushed back into the early industrial period which, for example, has allowed an estimate of the large-scale anomalies following the eruption of Mount Tambora in 1815 (Brohan et al., 2016). Data assimilation techniques are also used to obtain 3-D reconstructions further back in time (e.g., Franke et al., 2017; Tardif et al., 2019).

Using early records in analysis of mechanisms as well as detection and attribution requires careful treatment of missing values and consideration of data coverage, usually limiting the analysis to data-covered areas in both observations and climate models. This avoids, at least to some extent, introducing biases due to uneven distribution of data across the globe (e.g., limited coverage in high latitudes, Cowtan et al., 2015); and also circumvents relying on assumptions made in infilled datasets. Estimates of data uncertainty are important in order to evaluate how they translate into the uncertainty of specific findings based on these data (Morice et al., 2012).

Some of the results presented here rely on widely used detection and attribution methods. These have been recently reviewed (e.g., in Bindoff et al., 2014) and are only briefly outlined here. The regression-based detection and attribution method used here assumes that an observed climate change **y** is regarded as a linear combination of externally forced signals **X** and residual internal climate variability **u**, where **X** is an $m \times n$ matrix with each of the m columns a separate fingerprint of dimension n, that captures the expected time-space pattern of change in response to a combination of m individual forcings. These include typically greenhouse gases, other anthropogenic factors (such as aerosols) and natural forcing ($\mathbf{X}_i$, i=1..m=3) (e.g., Hasselmann, 1997; Ribes et al., 2013):

1) $$\mathbf{y} = \mathbf{X}\mathbf{a} + \mathbf{u} \quad .$$

This equation assumes that forcings superimpose linearly. Linearity has been queried, and does not apply while under radiative imbalance (Goodwin, 2018). Also, feedbacks can change with the climate state. On the other hand, the nonlinear effect of radiative imbalance over the historical period should be small outside the immediate aftermath of strong eruptions; and swamped by large climate variability. Consistently, linearity has been found appropriate for large-scale changes in temperature across the historical period (Shiogama et al., 2013) and, along with a large body of work, we assume it here. **y** represents the observed record, usually after distilling it into a small-dimensional space n. This can be done by truncating to a limited number of Empirical Orthogonal Functions (Hasselmann, 1997; Hegerl et al., 1996; Tett et al., 1999) or using only few spatial indicators such as global mean temperature, hemispheric contrast and summer/winter contrast (Schurer et al., 2018). The outcome of the analysis is a vector of m scaling factors **a** that adjusts the amplitudes of each fingerprint to best match observations.

Fingerprints are usually derived from coupled climate model simulations, often by averaging across simulations from multiple models in order to both reduce noise from internal climate variability and to average across model uncertainty (the multi-model mean). Uncertainties in **a** are estimated by accounting for the effect of climate variability on **y**, usually using samples from climate model control simulations. When the uncertainty range around a fingerprint's scaling factor a_i is statistically separated from zero, the fingerprint i is detectable, and where it is significantly smaller or larger than '1' the best-guess response in observations is significantly smaller or larger than in the models. **X** may contain noise if, for example, it arises from averaging across a limited number of climate model simulations. In this case a total least square regression may be applied (Allen and Stott, 2003), which also accounts for noise in **X** in the calculation of **a** and its uncertainty. Also, different climate models may simulate a different response to forcing leading to uncertainty in **X** which can lead to uncertainty not captured in standard methods (Hannart et al., 2014; Schurer et al., 2018). The latter study found that the widespread practice of inflating (in the specific case, by a factor of 2.6) the climate model variance approximately removes overconfidence in results for large-scale temperature, and so we apply it here for simplicity.

Process studies from climate model simulations can provide powerful evidence for how forcing may have influenced climate, even if links cannot be demonstrated in observations based on detection and attribution, for example, in regions of low signal-to-noise ratio. In Section 3 we show some results for the likely contribution of aerosols to regional climate based on modelling.

Another important cause of climatic fluctuations is variability generated within the climate system, either by atmospheric or ocean dynamics, or their interaction. Detection and attribution work considers this variability generally as 'noise'. However, some approaches quantify the effect of modes of variability directly, as is done for example using the Cold Ocean Warm Land pattern (Wallace et al., 1995). In the present paper we give some examples showing how decadal or multidecadal temperature fluctuations can arise from (probably) random long-term tendencies in the North Atlantic Oscillation and the ocean response to it.

3. Role of Forcings in large-scale climate change over the instrumental period

a) Observed and simulated global-scale changes in temperature

The 19th century began as one of the coldest periods of the last millennium, at least for the Northern Hemisphere (see Masson-Delmotte et al., 2013), following a slightly warmer 18th century (Figure 1). Some of the coldest observed periods followed in the two years after the powerful eruption of Mount Tambora in 1815 (Raible et al., 2016). After that, temperatures began to show a slow rise, interrupted by cooling induced by volcanic eruptions in the 1830s (Brönnimann et al., 2019a) and then the Krakatoa eruption in 1883 (see figure 1). Global temperatures rose particularly rapidly over the early 20th century, showing anomalous warming from the 1920s through the 1940s (see Figure 1; and Hegerl et al., 2018), before plateauing in the 1950s and 60s, and beginning their strong ongoing increase.

Much of this temperature variability has been driven by external forcing (Figure 1): following a small dip of CO_2 in the Little Ice Age (Masson-Delmotte et al., 2013; Schmidt et al., 2012), CO_2 began to rise since the beginning of industrialization along with other greenhouse gases. The strongest increase in radiative forcing by greenhouse gases occurred in the recent few decades, an increase that is steadily continuing to date. With the burning of fossil fuels, anthropogenic aerosols began to increase as well, with aerosol forcing estimates peaking globally around 1980, although emissions have continued increasing in South and East Asia while decreasing in Europe and North America since then.

Natural forcing has imposed decadal scale variations on the total forcing (Figure 1): While global radiative forcing by solar irradiance variations was quite small, with an increase towards the mid-20th century and a minimum in the 17th and early 19th centuries, episodic volcanic eruptions caused periods of stronger or weaker than average negative forcing. The largest was the eruption of Mount Tambora in 1815, which came shortly after an eruption of unknown origin in 1808 or 1809 (Cole-Dai et al., 2016; Guevara-Murua et al., 2014; Raible et al., 2016). A strongly smoothed version of the total forcing (anthropogenic and natural forcings combined) deviates from the anthropogenic forcing substantially over some periods, most notably, the period around the Tambora eruption, and the mid-20th century. The latter is largely due to a hiatus in volcanism. It has been argued that volcanic eruptions only cause short-term cooling. However, climate model simulations show an extended cold period following the 1809/Tambora period, with no single year in model simulations with

HadCM3, for example, reaching the average of the 20 years prior to the eruptions up to the 1830s (Schurer et al., 2014), when another period of volcanism kept temperature low until the 1840s (Brönnimann et al., 2019a). Equally, climate models simulate long-term warming in periods with little volcanic forcing, such as the early 20th century (Hegerl et al., 2018). The climate model simulated response to all forcings combined (multimodel mean, concatenated between Coupled Model Intercomparison Project Phase 5 (CMIP5) and Paleoclimate Modelling Intercomparison Project (PMIP) simulations, see methods; Figure 1c) closely follows the forcing and replicates the observed and reconstructed global temperature estimates largely within uncertainties. Some studies have argued that the response to forcing could account for more of the observed global variability if its uncertainty is taken into consideration (Haustein et al., 2019).

The observations deviate from the model mean and range during some periods, the first of which is 1900-1910. This was a period of anomalously cold SST conditions developing in the South Atlantic and spreading northward (Hegerl et al., 2018). Both long-term homogeneous stations in southern Africa and South America as well as ship data support the anomalously cold conditions during this period, which clearly deserves more attention (see discussion of ocean below). Observations are warmer than models during the peak of the early 20th century warming around 1940, which was particularly pronounced in the Arctic and Atlantic sector (Brönnimann, 2009; Hegerl et al., 2018; Wood and Overland, 2010). The most recent deviation between climate models and observations occurred during the 'hiatus' of warming from around 1998 to 2012 (Figure 1c; Lewandowsky et al., 2016; Medhaug et al., 2017; Yan et al., 2016) which has since ended with global warming rapidly resuming (Hu and Fedorov, 2017).

The spatial pattern of observed trends (Figure 2) shows that both warming and cooling/flat periods can show distinctly different spatial signatures. A trend towards cool conditions in some regions prior to 1910 shows also relatively cool conditions in data covered parts of the Southern Ocean. The early 20th century warming emerges from this cold period (Figure 2b), which is equally strong or stronger over ocean and, while it started with strong Arctic and North Atlantic warming (Hegerl et al., 2018), it is relatively uniform for the 1910-1950 trend. From 1950 to 1980, observations show a hemispherically asymmetric spatial trend pattern, with more regions warming in the Southern Hemisphere and some oceanic regions of cooling in the Northern Hemisphere (Figure 2c). From 1980 onwards, a strong warming emerges that is almost global in nature with very strong trends (Figure 2d). Exceptions are the off-equatorial and tropical regions of the central and eastern Pacific associated with the transition to a negative Interdecadal Pacific Oscillation (IPO) phase (Power et al., 1999; Zhang et al., 1997) coincident with the early-2000s hiatus (England et al., 2014; Kosaka and Xie, 2013), and the high-latitude Southern Ocean (Armour et al., 2016; Jones et al., 2016).

b) Causes of global-scale changes in temperature

What caused these spatially diverse long-term trends? The similarity between simulated and observed/reconstructed changes in Figure 1 suggests a strong role of external forcing. Detection and attribution methods are able to disentangle which of the forcings have played key roles in observed changes, and which are less important. Table 1 summarizes published global and hemispheric scale detection and attribution results from various timelines. Analysis of palaeoclimatic records for hemispheric and global mean data suggests that significant trends in response to greenhouse gas increases can already be detected and attributed by 1900, both across the Northern Hemisphere and in some regions such as Europe (Hegerl et al., 2011; PAGES 2k Consortium et al., 2013; Schurer et al., 2014). This result is based on an analysis that captures the time evolution of hemispherically averaged temperature from the 15th century (Table 1) and hence captures both the temperature response to a sustained, small CO_2 drop over parts of the Little Ice Age (Koch et al., 2019) and the

response to the CO_2 increase following industrialization. Abram et al. (2016) also found sustained warming in regional proxy-reconstructions from the early mid-19th century, consistent with climate modelling.

However, volcanism is important over much of the 19th century as well: Figure 1d illustrates that in models, the warming period up to the eruption of Krakatoa was in large parts a relaxation from a period of heavy volcanism around the Mount Tambora eruption (Brönnimann et al., 2019a). From the 50-year trend centred around 1860 onwards (ending around 1885; Figure 1d), climate models indicate that the warming trend originating from the recovery after heavy volcanism is exceeded by the warming trend caused by greenhouse gas increases. Detection and attribution analyses (Table 1) confirm detectable responses to both forcings.

Analyses over the entire *instrumental period* robustly detect the influence of greenhouse gases when using fingerprints that are derived by averaging across many available climate models. Results based on fingerprints from individual models can vary more, with separate detection of greenhouse gas responses in an analysis simultaneously estimating natural, greenhouse gas and aerosol forcing only in about half of the models (Gillett et al., 2013; Jones et al., 2013; Ribes and Terray, 2013). However, integrating attribution results across model uncertainty in a Bayesian analysis yields a robustly detectable greenhouse gas signal even in the presence of model uncertainty (Schurer et al., 2018). The response to other anthropogenic forcings, particularly from aerosols, is less clearly detectable unless prior assumptions exclude very large or negative responses (Schurer et al., 2018) and their role in regional anomalies is discussed below (see also Table 1; Bindoff et al., 2014).

Both for reconstructed palaeoclimate and climate over the instrumental period, the response to natural forcing (solar and volcanic combined) is robust across studies, although the best estimate magnitude is only about 70% of that in climate model simulations (see also Figure 3, scaling factors in the top panel indicate the best fit and uncertainty range of the magnitude of the model simulated pattern to observations; **a** in eqn. 1). In instrumental data this slightly smaller response to natural forcing may, at least in part, be due to the confounding effect of El Niño events in the later 20th century following eruptions which, when accounted for, brings models and observations in closer agreement in attribution studies (Lehner et al., 2016). A strong role for volcanism in decadal temperature variability is confirmed in detection and attribution studies for the last millennium (Table 1; see Bindoff et al., 2014; Schurer et al., 2014) although again the amplitude of detected changes appears smaller in reconstructions than model simulations. Volcanism has also been implicated in long-term hiatus and surge events of global warming (Neukom et al., 2019; Schurer et al., 2015).

Only few studies are available that estimate the role of solar forcing alone. Over the last five centuries, reconstructions support only a moderate magnitude of solar forcing (Schurer et al., 2014), as do analyses of the instrumental period based on formal attribution (Benestad and Schmidt, 2009; Stott et al., 2003) and global time series regression analyses (Folland et al., 2018; Lean, 2018). Analysis also suggests a role of solar forcing in trends (Figure 1d), although it is not significant against internal variability in climate models (indicated by the spread of simulations) yet may have slightly influenced trends. The solar influence may be stronger on regional climate where solar forcing may influence modes of climate variability. For instance, during solar minima, there appears to be an increased likelihood of the negative phase of the North Atlantic Oscillation and increased North Atlantic/Eurasian blocking frequency (Lockwood et al., 2010), linked with cold winters in Europe and warm ones in Greenland (e.g., Gray et al., 2016; Ineson et al., 2011; Scaife et al., 2013; Woollings et al., 2010). Possible effects have also been found on equatorial Pacific SSTs, sea level pressure in the Gulf of Alaska and the South Pacific, the strength and location of tropical convergence zones, the

strength of the Indian monsoon and the location of the descending branch of the Walker circulation, impacting on precipitation (Bindoff et al., 2014; Gray et al., 2010 and references therein; Meehl et al., 2009). These hypothesized effects may either arise through SST influences, or through solar influence on the stratosphere (Gray et al., 2010), and remain uncertain.

Figure 3 shows the implications of detection and attribution of greenhouse gas, other anthropogenic, and natural forcings over the instrumental period on causes of the trends over the periods shown in Figure 2 (note that the results shown are from Schurer et al., (2018) but are qualitatively and quantitatively similar to those in other studies, Table 1). The attribution analysis is based on a multimodel mean fingerprint over the instrumental period, with uncertainties enlarged to avoid overconfidence (by increasing the variance of the control simulation by a factor of 2.6, see methods and Schurer et al., 2018). It yields a well-constrained greenhouse gas response that is consistent and close in magnitude to the multi-model mean response in climate models. It also shows a detectable response to natural forcing, which is slightly smaller in observations than in climate models (Figure 1, yellow). The response to other anthropogenic forcing is more uncertain and depends on prior assumptions (Figure 3a, the informative prior assumes no negative scaling factors and decay at about 3, peaking at 1 while the flat noninformative prior covers a -1 to +3 range).

These attribution results can be interpreted as observation-based estimates of the contribution of forcing to different periods, in a similar way that the IPCC has estimated the greenhouse gas contribution to the recent 60 years (Bindoff et al., 2014). This is done by inflating or deflating the multi-model mean forced contribution to a period within the range of the estimated scaling factors. Note that interpreting the results of the long analysis over shorter segments carries additional uncertainties in that errors in the time evolution of the response may impact shorter periods, yet average out over longer periods. Where this occurs, uncertainties over the shorter period may be larger than indicated by the scaling factor uncertainty only.

Results show that the observed cooling from 1870-1910 in observations (uncertainty in observed change expressed in grey histogram; Morice et al., 2012) occurred despite a small greenhouse forced warming, and appears to be due to a combination of internal climate variability, natural forcing (e.g. Mount Krakatoa eruption) and aerosols. The noticeable contribution by greenhouse gases is consistent with the early detection of greenhouse warming from proxy-based data discussed above. This period shows stronger cooling than simulated, consistent with the above discussed period of anomalously cold SSTs in the very early 20th century. The subsequent period (Figure 3c) is dominated by the early 20th century global warming trend. The combined response to anthropogenic forcing (purple) is smaller than the observed trend, indicating a role of internal climate variability in the warming to 1950 (see also Hegerl et al., 2018). The detection and attribution results further suggests that the plateau in observed trends from 1950-1980 occurred despite a net positive anthropogenic forcing, which is a strong greenhouse warming counteracted in large part by very strong aerosol induced trends. The analysis indicates that this net anthropogenic forcing was counteracted by slightly negative natural forcing (e.g. eruption of Mount Agung). Subsequently, greenhouse gases caused a strong warming trend from 1980-2012 (when CMIP5 simulations end); with the aerosol influence weakening and largely counteracted (in best estimate) by a slightly positive response to natural forcing, which is consistent with the eruption of El Chichón (1982) and Mount Pinatubo (1991) in the first half of the period (see also Figure 1d).

These results, particularly, the varying contribution of natural forcings to different decades across the industrial periods as well as the early detectable greenhouse gas influence illustrates the difficulty of finding a suitable and 'typical' pre-industrial period (Hawkins et al., 2017; Schurer et al.,

2017): Periods are influenced differently by natural forcing, and CO_2 has been rising since 1750, following the enigmatic drop (Koch et al., 2019) around the Little Ice Age. Therefore there is no constant and unambiguous preindustrial background temperature. Figure 1 shows that the period 1850-1900 (which is frequently used as proxy for the pre-industrial baseline due to the availability of instrumental observations with some global-scale coverage; Allen et al., 2018) is a fairly stable climatic period with only small trends superimposed on the anthropogenic forcing, which, however, by that time had already caused a warming trend.

c) The role of anthropogenic aerosols in regional changes

Model simulations and attribution results suggest that aerosols have been playing a key role in shaping regional climate, over the entire 20th century and maybe before. It has been argued that small aerosol perturbations in early industrial time may have caused substantial impacts in a less polluted atmosphere (e.g., Carslaw et al., 2013) - with potential consequences for our best estimate of aerosol radiative forcing (Booth et al., 2018; Kretzschmar et al., 2017; Stevens, 2015). This is, however, difficult to quantify as the natural aerosol loading due to biomass burning and natural sources is uncertain, as is the magnitude of aerosol-cloud interactions and therefore the realistic nature of their representation in models (e.g., Toll et al., 2017; Wilcox et al., 2015; Zelinka et al., 2014).

Long-term aerosol impacts on regional climate are supported by climate modelling (Figure 4). European mean surface temperature, similar to global temperature, shows a plateau in warming at the period of strongest European and North American aerosol emissions that is reflected in aerosol only simulations, but not in greenhouse gas or natural only runs (Figure 4a). Furthermore, the observed daily temperature range over Europe has decreased throughout that time period, although with quite strong variability and data uncertainty. Comparison with surface solar radiation (e.g., Makowski et al., 2008; Wild et al., 2007), and single-forcing simulations (Figure 4b; Undorf et al., 2018b) suggest a contribution from anthropogenic aerosols to this decrease. While the temperature impact of aerosols is expected to have been largest over their emission regions, and downstream thereof (e.g., Shindell et al., 2010), the global, heterogeneous patterns of temperature change simulated by models (e.g., Shindell et al., 2015; Wang et al., 2016) suggest relevant impact elsewhere, too. Aerosol impact on other variables is mediated by the change in temperature, as suggested for Arctic sea ice (e.g., Acosta Navarro et al., 2016; Mueller et al., 2018), or by temperature gradients, like the inter-tropical convergence zone (ITCZ; Chang et al., 2011; Hwang et al., 2013; Undorf et al., 2018c; see also Figure 8a,b) and the strength and position of the Northern Hemisphere subtropical jet stream and the tropical belt width (e.g., Allen and Ajoku, 2016; Undorf et al., 2018b).

Long-term variability in the monsoons has also been linked to aerosol forcing, in East Asia (Guo et al., 2013; Li et al., 2016), South Asia (e.g., Bollasina et al., 2011; Guo et al., 2015), and Australia (Rotstayn et al., 2012; Dey et al., 2019) as well as over the Sahel (e.g., Ackerley et al., 2011; Dong et al., 2014; Held et al., 2005; Rotstayn and Lohmann, 2002). In particular the decrease between the early to mid-20th century and the 1980s and the subsequent recovery in precipitation over the global land surface (Wilcox et al., 2013) and global-scale monsoon precipitation, averaged across Asian, African, and American monsoon regions in the Northern Hemisphere, has been attributed to aerosol forcing (Polson et al., 2014). The aerosol influence on monsoon precipitation changes in South Asia (Figure 4c) was found to be driven by a combination of emissions from North America, Europe and South Asia that are all simulated to weaken the monsoon circulation (Undorf et al., 2018c). North American and European aerosols, along with natural forcings, are detectable drivers for African monsoon precipitation, but the model simulated changes over this region appear weak compared to observed

changes, a source of concern about both modelling future changes and understanding monsoon variability (Biasutti, 2013; Polson et al., 2014). The dominant mechanism by which the aerosol impact is mediated, on the other hand, seems to be related to shifts of the ITCZ and is as such a well-studied response to aerosol-induced changes of the interhemispheric temperature gradients (Chang et al., 2011; Chiang and Friedman, 2012; Hwang et al., 2013; Undorf et al., 2018c; see also Figure 8a,b). Related impacts have been suggested on other large-scale atmospheric circulation features like the strength and position of the Northern Hemisphere subtropical jet stream and the tropical belt width (e.g., Allen and Ajoku, 2016; Undorf et al., 2018b).

d) Changes in global-scale precipitation

Global warming will affect the global water cycle and has probably already done so (IPCC, 2013). Diagnostics of atmospheric water content and humidity, while showing clear anthropogenic signals (see Bindoff et al., 2014; Santer et al., 2007) only go back through the satellite era. There is evidence from the mixed satellite/in situ record that the expected intensification of the hydrological cycle with wet regions getting wetter and dry getting drier is indeed detectable, although only if tracking wet and dry regions with the seasonal cycle and over time (Polson et al., 2013; Polson and Hegerl, 2017). In situ rainfall stations are able to support a longer time horizon, but are spatially sparse, fairly uncertain and only available over land (Harris et al., 2014; Zhang et al., 2007). However, over land precipitation is influenced by a complex combination of SSTs, land use influences, land-sea contrast and direct forcing (Greve et al., 2014), and future changes over land are hence uncertain and strongly model dependent (IPCC, 2013). Furthermore, climate model simulations indicate that over the historical period, precipitation changes over land are moderated by other forcings, particularly shortwave forcings (e.g., Richardson et al., 2018). Nevertheless, since the second half of the 20th century, a human induced increase in intense precipitation has been detected, consistent with a moister, warmer atmosphere (Min et al., 2011; Zhang et al., 2013). Similarly, there is some evidence from in situ data over the second half of the 20th century that the high latitudes are becoming wetter (Min et al., 2008) although data uncertainty here is substantial (Hegerl et al., 2015). Zonal land precipitation shows a change since the 1920s that is broadly consistent with the expected response to anthropogenic forcing (Zhang et al., 2007), although particularly seasonal responses are uncertain and noisy (Polson et al., 2013; Sarojini et al., 2012). Drought atlases from proxy data and instrumental data support a long-term change in drought frequency with a detectable human influence by the middle of the 20th century (Marvel et al., 2019). While it remains to be seen to what extent this reflects precipitation change and to what extent increased evaporation due to warming, it provides powerful evidence that greenhouse gases have influenced aspects of the water cycle early on.

In contrast to changes over land, model-simulated precipitation changes over ocean are fairly robust across models, with a signal of wet regions getting wetter and dry regions getting drier. Many precipitation records over islands go back to the 1920s. While they are too sparse to constrain global precipitation changes, the island stations are able to evaluate the pattern of precipitation change associated with global temperature changes: The so-called precipitation sensitivity diagnoses the precipitation response to warming (for any reason including greenhouse gas induced warming) and is expressed as the change [%] in mean precipitation per degree of global mean warming. It has also been found to be a useful constraint on future changes if applied to extremes (O'Gorman, 2012). Island stations support a pattern of precipitation sensitivity that is in fairly good agreement with historical simulations from climate models (Figure 5) and shows a stronger correlation with historical simulations over the period since 1930 than with satellite data over the period since 1979 (Polson et

al., 2016). This both supports the simulated large-scale precipitation response and emphasizes the need for long records for noisy precipitation signals. An amplification of the global hydrologic cycle is also supported when using sea surface salinity as an "indirect rain gauge" (Schmitt, 2008; Terray et al., 2012): globally from the 1950s (Durack et al., 2012; Skliris et al., 2014) and over the Atlantic from the early 20th century onwards (Friedman et al., 2017).

Forcing is also expected to directly affect rainfall through a change in energy available for evaporation. Such a response leads, at least in models, to a rapid precipitation decrease after volcanic eruptions over land (Iles et al., 2013; note that instrumental records are too noisy to evaluate this response). The response to greenhouse gas induced warming is muted compared to that to aerosols since changes in lapse rate and atmospheric energy budget constraints reduce the precipitation response to warming (Allen and Ingram, 2002; Andrews et al., 2010; Bala et al., 2010; Cao et al., 2012; Lambert and Allen, 2009; O'Gorman, 2012). This is why the global land response to shortwave forcing such as that from anthropogenic and volcanic aerosols may be more detectable over the historical period than that to greenhouse gas increases (Allen and Ingram, 2002). Long-term streamflow data are an excellent opportunity to study the watercycle response to forcing. Several large rivers have streamflow records back into the 19th century. These may reflect changes in response to a combination of precipitation and evaporation, possibly including CO_2 induced changes in transpiration (Gedney et al., 2006; Piao et al., 2007), and can be affected by human influences including irrigation, land use changes, dam construction, and extraction (Dai, 2016; Dai et al., 2009; Gerten et al., 2008). However, they show a detectable and more robustly observed short-term response to volcanic eruptions, with drying on average in the wettest regions of the planet, detectable in the tropics and northern Asia, and detectable wettening in some dry regions such as the southwestern US (Iles and Hegerl, 2015).

4. Variability generated within the climate system

In this section we discuss some long-term climate changes that are linked to long-term tendencies in modes of climate variability. It is recognized that external forcing may change the preferred direction and location of modes of climate variability, which is an important uncertainty in future climate change (Shepherd, 2014). However, such changes are hard to detect among high circulation variability, hence we only discuss changes caused by trends in circulation, not its causes. At the end of the section, we briefly discuss an example that illustrates why it is difficult to conclude with confidence whether large-scale temperature variability in climate models is consistent with observations.

a) Circulation related to atmospheric or coupled variability

Long-term changes in atmospheric circulation are best documented for the Northern Hemisphere Atlantic sector. Here, the North Atlantic Oscillation (NAO) is the dominant mode of variability at the surface, and related to variations in storm tracks, particularly, in the winter. The NAO is often defined by the pressure difference between the Icelandic low and the Azores High (e.g., Hurrell, 1995), has a distinct spatial pattern of sea level pressure (e.g., Hurrell and Van Loon, 1997) and has been observed over a long period of time (Hurrell et al., 2003). The NAO is closely related to the Northern Annular Mode (Thompson and Wallace, 2001) which is more zonal in nature and links to variations in the polar stratospheric vortex. Due to the longer record, we focus here on the NAO over the Atlantic Sector (Hurrell and Deser, 2009). While the NAO is fairly white on timescales longer than interannual, it shows some long-term trends over the period of record. After a variable period

with no pronounced trend in the second half of the 19th century, the NAO increased and then showed a marked longterm decrease between the early 20th century and the 1970s. This was followed by a strong upward trend peaking in the 1990s and then a downward trend into the so-called hiatus period (e.g., Hurrell, 1995; Iles and Hegerl, 2017; Thompson and Wallace, 2001) . Winters with an anomalously high NAO index tend to be warmer over Eurasia and anomalously cold in eastern North America and parts of Greenland as well as of the North Atlantic (Figure 6, central panel middle). The opposite is true for low NAO values (Hurrell and Van Loon, 1997; Iles and Hegerl, 2017; Figure 6, central panel left and right). If this linear relationship holds for trends in the NAO (and aggregates of NAO trends from climate models suggest it does; Deser et al., 2017; Iles and Hegerl, 2017) then NAO trends cause long-term temperature changes (Figure 6). The NAO decrease to the 1970s may have led to dynamically induced boreal winter trends counteracting greenhouse warming to 1970, then strengthening it to the 1990s, and then counteracting it again. Residual trends, after linearly removing the NAO influence, show a more uniform warming pattern (Figure 6 bottom; see also Thompson and Wallace, 2001). Not shown is the impact of the NAO on precipitation, which would lead to expected rainfall trends of opposite sign over the Mediterranean and Northwest Europe (Deser et al., 2017). Note that based on climate model simulations the ocean response to the NAO trend may enhance the response relative to that estimated from the interannual relationship (see next section; see also Deser et al., 2017; Iles and Hegerl, 2017 for regression/composite based results).

The zonal mean Hadley Circulation is the globally dominant circulation feature, and changes in its location and strength could potentially have large impacts, particularly, on rainfall. Interannual variability in the strength of the Hadley Circulation, as well as its relationship to the El Niño-Southern Oscillation is well studied, but trends in its strength are not well established (Nguyen et al., 2012). Nevertheless, a robust widening of the tropical belt is found since ca. 1980 (although reanalyses data sets tend to overpredict the widening; see Davis and Davis, 2018). Although climate models predict a widening due to greenhouse gas forcing and also a response to hemispherically heterogeneous aerosol forcing (Section 3c), internal variability is high and yet precludes attribution (Staten et al., 2018). The widening from 1980 onward started from a southward shifted state: The northern tropical belt shifted southward from the 1940s to 1980 (Brönnimann et al., 2015), and similar decadal changes in the edge of the northern tropical belt have also been found in earlier periods in tree-ring based reconstructions (Alfaro-Sánchez et al., 2018).

Furthermore, a weakening of the Pacific Walker circulation was suggested at a centennial scale since the mid-19th century, in line with model simulations (Vecchi et al., 2006). However, observations from recent decades point to a strengthening. Apart from data issues, this strengthening might have been due to internal variability, which is a dominant factor controlling the strength of the Pacific Walker circulation (Chung et al., 2019). The Walker circulation is closely linked to El Niño, the climate mode with largest global influence, which again shows substantial variability in its variance on multidecadal timescales (Wittenberg, 2009). Thus, the contribution of changes in circulation to observed long term changes in precipitation and temperature remains uncertain, as is a possible role of forcing in these changes. This remains a research priority.

b) Response and role of ocean and sea ice

The biggest potential source of decadal climate variability is the ocean. Even an inert ocean would cause decadal climate variability by integrating weather noise, and ocean dynamics are expected to enhance this variability (Frankignoul and Hasselmann, 1977; Hasselmann, 1976). For example, in the GFDL model, a warming episode similar to the early 20th century warming occurred in a historical simulation due to ocean overturning variability (Delworth and Knutson, 2000). Figure 7 shows

another example based on the Max-Planck Institute ocean model forced by century-long reanalysis ERA20C (Poli et al., 2016) with an experimental set up similar to Müller et al. (2015). Surface temperatures in the North Atlantic are closely associated with a downward ocean surface heat flux (latent plus sensible heat flux) on an inter-annual timescale (Figure 7b) and upward into the atmosphere heat flux on decadal to multi-decadal timescales (Figure 7c, see also Gulev et al., 2013). This clearly indicates a short-term ocean response to atmospheric forcing such as by the NAO and a long-term memory (sub-decadal to multi-decadal) by ocean inertia resulting in heat release back into the atmosphere. In fact, the role of wind-driven forcing, such as that linked to the NAO, for the ocean inertia has been widely been documented (e.g., Delworth and Mann, 2000; Eden and Jung, 2001; Eden and Willebrand, 2001). Sub-decadal to decadal variations appear in the coupled North Atlantic climate system following wind forcing and a damped oscillation (Czaja and Marshall, 2001; Eden and Greatbatch, 2003). Further multi-decadal variations in the North Atlantic are closely associated with buoyancy-forced deep convection (Bersch et al., 2007) and the complex interplay between processes in higher latitudes and the North Atlantic (Jungclaus et al., 2005; Polyakov et al., 2010).

The variations of the NAO, North Atlantic heat fluxes and SST underwent strong multi-decadal variations (Figure 7d) linked to the trends in the NAO discussed above. Similarly, albeit with a delay of a decade, the SST show a cooling period during the 1960s and 1970s flanked by warming periods 1920s-1930s and 1990s-2000s, respectively. The warming period in the 1920s has led to a mean increase of surface air temperature (>0.5°) within the basin and adjacent continents (e.g., Brönnimann, 2009) and has the largest effects in high latitudes (Johannessen et al., 2004). Changes in the atmospheric circulation have been suggested as a primary precursor of the warming (e.g., Polyakov et al., 2010). In fact, by forcing an ocean model with century-long reanalysis data it has been shown that the NAO-like atmospheric circulation induces anomalous northern heat transport in the North Atlantic incites an Arctic warming with a delay of about a decade (Müller et al., 2015). North Atlantic wind anomalies may have contributed to an increased transport of warm waters into higher latitudes and to Arctic warming (Bengtsson et al., 2004), contributing a signal of internal variability to the early 20th century warming. Figure 7e,f underlines the importance of the heat transport for the heat release in the North Atlantic and higher latitudes. Variations of the heat transport and the Atlantic Meridional Overturning Circulation (AMOC; here 26°N and 1000 m depth) reveal the close temporal relationship to the NAO, SST and heat fluxes.

This strong ocean/coupled dynamics hypothesis contrasts with the possibility that some observed SST variations in the Atlantic may be linked to aerosols (e.g., Bellomo et al., 2018; Booth et al., 2012; Haustein et al., 2019; Murphy et al., 2017; R. Zhang et al., 2013). Figure 4d illustrates strong AMV variability, but a downturn around 1970 that also occurs in response to historical forcing, suggesting that the AMV is not purely an internal mode of climate variability. Single-forcing simulations indicate a role for both anthropogenic aerosol and natural forcing (Figure 4d), the latter of which has also been suggested to have played a role during the last millennium based on proxy records (Knudsen et al., 2014; Wang et al., 2017) and model studies (Otterå et al., 2010). The connection of the AMV to ocean variability is unclear, with some evidence pointing to a contribution from a forced component of the AMOC (e.g., Tandon and Kushner, 2015; Undorf et al., 2018a; Watanabe and Tatebe, 2019) in response to natural and anthropogenic aerosols (Cowan and Cai, 2013; Delworth and Dixon, 2006; Menary et al., 2013). Determining the contribution by forcing and climate dynamics to decadal ocean variability, particularly in the Atlantic, therefore remains uncertain and requires more attention and, probably, a longer data horizon.

Ocean variability has also been implicated in the recent slowdown period of warming: Periods with decadal warming or cooling due to natural or internal variability that is strong enough to double or counteract present anthropogenic warming are dispersed throughout the historical record (Fyfe et al., 2016; Schurer et al., 2015). Volcanic forcing is a pacemaker particularly for long periods of fast and slow warming, with cooling due to eruption effects and rapid warming during recovery (Schurer et al., 2015). However, hiatus and surge periods occur also due to internal climate variability and show a pattern involving the tropical Pacific oceans (Roberts et al., 2015), with possibly a contribution by the Atlantic in observations (Schurer et al., 2015).

Sea ice responds to ocean and atmospheric temperatures, with decreases in sea ice not only observed recently, but also during the early 20th century high latitude warming (Titchner and Rayner, in preparation; Walsh et al., 2017). For example, large changes in the sea ice conditions around Spitsbergen were reported in the 1920s and attributed to additional warm water being pushed north by the Gulf Stream (Ifft, 1922). For the recent period since 1953, signals of greenhouse gas, aerosol and natural forcing induced changes have been detected in the observations (Mueller et al., 2018). Notz and Stroeve, (2016) have suggested that summer Arctic sea ice is melting proportionally to cumulative carbon emissions, although other studies have proposed a role for internal variability in the recent decline (e.g., Day et al., 2012). Knowledge of pre-1950s Arctic conditions could be substantially improved through the digitisation of many decades worth of voyager records along with thousands of logbooks(e.g., García-Herrera et al., 2018). These logbooks contain instrumental observations of temperature, pressure and winds, and often include information on sea ice extent back to the 19th century.

c) Is decadal climate variability realistic in climate models?

The climate variability simulated in models is the yardstick against which attribution of change to causes occurs. Climate variability has also been identified as a potential emergent constraint on climate sensitivity, which is theoretically supported by the fluctuation dissipation theorem (Cox et al., 2018). Both make it vital to evaluate if long observed records support the decadal variability simulated in climate models. This question has been addressed in multiple IPCC reports (e.g., Flato et al., 2013) and is illustrated here for the case of Northern and Southern hemisphere SST variability in in Figure 8, comparing two observational SST datasets, ERSSTv5 (Huang et al., 2017) and HadSST3 (Kennedy et al., 2011a; 2011b), and 10 CMIP5 models. The observations largely follow the multimodel mean and range in the historical forcing simulations over the 20th century, although some of the deviations particularly in the Southern Hemisphere are quite large, such as during the 1920s (Figures 8a-8b). There is also an excursion between models and data during the early 1940s that may be connected to biases related to the second world war (Haustein et al., 2019; Kennedy, 2014). The standard deviation of the residual SST variability (after subtracting the multimodel mean) is large in observations compared to that of the historical simulations, particularly for the Southern Hemisphere (Figure 8c).

To what extent this discrepancy is due to model error, residual forcing or remaining observational error in SSTs (Chan and Huybers, 2019; Haustein et al., 2019) is presently unclear (Friedman et al., in revision). The difference between variability with multimodel mean removed compared to that from control simulations (Figure 8c) suggests that residual forcing may have contributed to the variability in observations. However, there is a wide range of simulated variability amplitudes in the CMIP5 models, even on the global scale (Knutson et al., 2013; Schurer et al., 2013; Sutton et al., 2015). We conclude that, evaluating which, if any, of the climate models simulate reliable variability on decadal timescales is difficult – both due to limited sampling in observations, and the difficulty to separate forced response from internally generated variability. This should be a high priority for research.

5. Example of long-term changes on local weather variability

Lastly, the large-scale changes over the instrumental period also had a demonstrable impact on local weather variability that would have affected society and ecosystems. Individual extreme events occurred in the past, and their analysis and attribution is an area that is of developing interest. For example, the European 'year without a summer' had a clear impact from the Mount Tambora eruption which greatly enhanced the probability of such a cold summer as occurred in 1816 (Schurer et al., in press). The Dust Bowl heat waves in the central United States in the 1930s set records to date (Cowan et al., 2017; Donat et al., 2016), and have likely been strongly influenced by changes in land cover (Cowan et al., in prep.) consistent with sensitivity of land climate to vegetation and land degradation (Arneth et al., 2019). The 1947 European heat wave (Harrington et al., 2019) record was only superseded in 2003. Figure 9 illustrates that long-term changes are detectable even in day-to day variability: many record-cold winter temperatures that occurred early on in Uppsala, Sweden, would be considered extremely rare at present, while some recent warm temperatures were rare in the past, and the distributions of daily temperature diverge significantly (based on a Mann-Whitney U test) between the three analysis periods of the early 19th century, early 20th century and recent period. Almost for every day of the year for Central England, and for most of those for the Uppsala record, the day-to-day variability is significantly different today from what it was 200 years ago, and for about half the year the change between the early 20th century warm period and the present is significant. The Figure also illustrates the challenges of old records: The higher 90th percentile for peak summer values early on in the Uppsala record may possibly have been due to changes in instrument exposure (Moberg et al., 2003). Studying old record-setting events will help to better understand the magnitudes and feedbacks of climate variability and extreme events.

6. Synthesis and open questions

We have summarized that both external forcings and decadal climate variability have played a key role throughout the instrumental era. Greenhouse gas increase emerges as important throughout, supported by the analysis of proxy based data, and had already caused a detectable warming by 1900. The analyses also emphasize that the anthropogenic warming trend can be modified strongly both by natural forcing, and by climate variability, either on decadal timescales or due to decadal preferences of interannual modes, as here illustrated for the NAO. The period prior to 1950 contains strong variability (some of which may be realistic rather than data artefacts), cases of very strong natural forcing, and substantial changes in daily climate variability.

Hence the observed record in its full length contains vital information. It also has great potential to provide a constraint on future warming, and this has been used, for example, as one of several inputs to derive uncertainty ranges for IPCC predictions (Collins et al., 2014; Knutti et al., 2008; using the Stott and Kettleborough, 2002, approach) and recently in Goodwin, (2018) and Goodwin et al., (2018), generating observationally constrained projections. However, the power of attributed greenhouse warming for providing constraints is limited due to the still highly uncertain influence from other anthropogenic forcings, most notably, aerosols. Aerosols increased along with the burning of fossil fuels, yet burdens in Europe and North America noticeably decreased since the late 20th century, while continuing to increase in South and East Asia (Hoesly et al., 2018), with a global peak of sulphate aerosol emissions around 1980. Aerosols have likely influenced global temperatures with a heterogeneous pattern and larger changes near and downwind of their

emission regions, diurnal temperature range, and possibly even multi-decadal variability of the Atlantic as well as the large-scale atmospheric circulation. A particularly important impact of aerosols has been on monsoons and tropical rainfall. Land use change may be important as well, for example, on summertime extreme events (e.g., de Noblet-Ducoudré et al., 2012). Land use change is not necessarily realistically simulated in climate models (Pitman et al., 2009). For a more reliable attribution and prediction of regional scales, the inclusion of land use effects is vital and progress may arise from a CMIP6 modelling exercise Land Use Model Intercomparison Project (LUMIP; Lawrence et al., 2016).

Decadal modulation of greenhouse warming trends over the industrial period often involved natural forcings, particularly volcanism, which is able to drive periods of decadal and multidecadal warming and cooling trends. The contribution by volcanism to temperature trends is particularly pronounced in the early 19th century. The large response illustrates that strong volcanic forcing would have a considerable impact on future warming trajectories.

Instrumental records of precipitation change are only reasonably widespread since the 1920s (Zhang et al., 2007), and the signal-to-noise ratio for precipitation data is low and local variability high. Yet, if aggregated skilfully, long records have the potential to allow useful evaluation of the model simulated precipitation response, and the improvement of data coverage and a better understanding of long-term homogeneity will be helpful.

Analysis of the influence of circulation on observed trends shows a role of, possibly random, decadal modulation of modes of variability such as the North Atlantic Oscillation. While optimal detection should be able to reduce the influence of internal variability, rotating away from noisy spatial dimensions (Hasselmann, 1979) or prewhitening noisy data (Allen and Tett, 1999); in practice the limit on the space-time degrees of freedom that can be used in these methods is so severe that this advantage cannot fully be taken advantage of, even for recent methods (e.g., Ribes et al., 2017; Ribes and Terray, 2013). Hence reliance on statistics alone to filter out the influence of modes of variability on forced signals is not sufficient, and explicit analysis of changes in modes of variability is useful. Also, the question remains as to what extent variations in modes of climate variability are induced by external forcing. This is uncertain not only in response to anthropogenic factors, but also in response to natural forcings. For example, volcanic eruptions are expected to cause a tendency for a positive NAO response as well as a possible El Niño response (Khodri et al., 2017; Robock, 2000; Swingedouw et al., 2017), although the response can be quite noisy (Hegerl et al., 2011; Polvani et al., 2019). Similarly, the relationship between solar forcing and the NAO is not yet fully understood (Gray et al., 2010). Addressing the connection between external forcing and the response in modes of variability as well as circulation features is a priority, and one which may not be well addressed by the present generation of climate models (Shepherd, 2014). In the near-term, climate variability will have a strong imprint on the emerging climate change signal in many regions (Deser et al., 2017), and hence evaluation of this long term variability is crucial. A careful evaluation of data quality as well as climate model processes may, for example, help to determine whether the strong early variability in the Southern Hemisphere in observations is realistic.

In summary, the record of observed and reconstructed climate over the industrial period contains important information to challenge and evaluate climate model simulations. Even though data from the longer past are more challenging to work with due to their poorer spatial resolution as well as homogeneity issues, the gain is well worth the effort.

Methods:

Literature search

This review focuses largely on identifying answers to key research questions about the instrumental era from existing literature; involving a broad set of coauthors to cover it well, and it includes new results that are being published. Additionally, web of science searches have been conducted to ensure broad coverage, using the keywords:

'Detection and Attribution, global temperature'; using outcomes from 2012 onwards as IPCC WGI will have captured results prior to that. A further search term was '19th century global temperature change'.

Construction of Figure 1: Merging of PMIP and CMIP multimodel simulations

Global mean temperature in all simulations is calculated as a blend of surface air temperature over land and sea-surface temperature over ocean with full coverage. To account for a potential difference in the sensitivity of forcings in the multi-model-means (MMMs) drawing on a different ensemble of climate models, the last millennium MMM is regressed onto the CMIP5 MMM during the period of overlap using a total least squares regression (scaling factor 1.20). The last millennium MMM is then scaled by the regression factor and is re-normalised so that it has the same mean over the shared period 1861-1999 as the CMIP5 MMM, where the CMIP5 MMM is plotted as anomalies since 1961-1990.

Acknowledgements

This work has benefitted from fruitful discussions with Tom Delworth, Hugues Goosse, Philip Brohan, Debbie Polson, Massimo Bollasina, and Simon Tett. A.S., A.R.F., S.U., T.C., C.I. and G.H. were supported by the ERC funded project TITAN (EC-320691). A.S. and G.H. were further supported by NERC under the Belmont forum, grant PacMedy (NE/P006752/1), and G.H. was by the Wolfson Foundation and the Royal Society as a Royal Society Wolfson Research Merit Award (WM130060) holder and by the NERC-funded SMURPHS project. SB was supported by the ERC funded project PALAEO-RA (787574).

We acknowledge the World Climate Research Programme's Working Group on Coupled Modelling, which is responsible for CMIP, the climate modelling groups for producing and making available their model output, the US Department of Energy's Program for Climate Model Diagnosis and Intercomparison, and the Global Organization for Earth System Science Portals for Earth System Science Portals.

Data availability statement

Data sharing is not applicable to this article as no new data were created or analysed in this study. Graphs shown in the study are either based on studies published elsewhere, or derived from data publically available including from JASMIN (for CMIP5 results) and observational data providers. Derivation of graphs that are not directly from other papers is described in detail in the paper; but time series shown can be provided from the first author on reasonable request.

References

Abram, N.J., McGregor, H.V., Tierney, J.E., Evans, M.N., McKay, N.P., Kaufman, D.S., the PAGES 2k Consortium, Thirumalai, K., Martrat, B., Goosse, H., Phipps, S.J., Steig, E.J., Kilbourne, K.H., Saenger, C.P., Zinke, J., Leduc, G., Addison, J.A., Mortyn, P.G., Seidenkrantz, M.-S., Sicre, M.-A., Selvaraj, K., Filipsson, H.L., Neukom, R., Gergis, J., Curran, M.A.J., Gunten, L. von, 2016. Early onset of industrial-era warming across the oceans and continents. Nature 536, 411–418. https://doi.org/10.1038/nature19082

Ackerley, D., Booth, B.B.B., Knight, S.H.E., Highwood, E.J., Frame, D.J., Allen, M.R., Rowell, D.P., 2011. Sensitivity of Twentieth-Century Sahel Rainfall to Sulfate Aerosol and CO2 Forcing. J. Clim. 24, 4999–5014. https://doi.org/10.1175/JCLI-D-11-00019.1

Acosta Navarro, J.C., Varma, V., Riipinen, I., Seland, Ø., Kirkevåg, A., Struthers, H., Iversen, T., Hansson, H.-C., Ekman, A.M.L., 2016. Amplification of Arctic warming by past air pollution reductions in Europe. Nat. Geosci. 9, 277–281. https://doi.org/10.1038/ngeo2673

Alfaro-Sánchez, R., Nguyen, H., Klesse, S., Hudson, A., Belmecheri, S., Köse, N., Diaz, H.F., Monson, R.K., Villalba, R., Trouet, V., 2018. Climatic and volcanic forcing of tropical belt northern boundary over the past 800 years. Nat. Geosci. 11, 933. https://doi.org/10.1038/s41561-018-0242-1

Allen, M.R., Dube, O.P., Solecki, W., Aragón-Durand, F., Cramer, W., Humphreys, S., Kainuma, M., Kala, J., Mahowald, N., Mulugetta, Y., Perez, R., Wairiu, M., Zickfeld, K., 2018. Framing and context, in: Masson-Delmotte, V., Zhai, P., Pörtner, H.-O., Roberts, D., Skea, J., Shukla, P.R., Pirani, A., Moufouma-Okia, W., Péan, C., Pidcock, R., Connors, S., Matthews, J.B.R., Chen, Y., Zhou, X., Gomis, M.I., Lonnoy, E., Maycock, Tignor, M., Waterfield, T. (Eds.), Global Warming of 1.5°C. An IPCC Special Report on the Impacts of Global Warming of 1.5°C above Pre-Industrial Levels and Related Global Greenhouse Gas Emission Pathways, in the Context of Strengthening the Global Response to the Threat of Climate Change, Sustainable Development, and Efforts to Eradicate Poverty.

Allen, M.R., Ingram, W.J., 2002. Constraints on future changes in climate and the hydrologic cycle. Nature 419, 228. https://doi.org/10.1038/nature01092

Allen, M.R., Stott, P.A., 2003. Estimating signal amplitudes in optimal fingerprinting, part I: theory. Clim. Dyn. 21, 477–491. https://doi.org/10.1007/s00382-003-0313-9

Allen, M.R., Tett, S.F.B., 1999. Checking for model consistency in optimal fingerprinting. Clim. Dyn. 15, 419–434. https://doi.org/10.1007/s003820050291

Allen, R.J., Ajoku, O., 2016. Future aerosol reductions and widening of the northern tropical belt. J. Geophys. Res. Atmospheres 121, 6765–6786. https://doi.org/10.1002/2016JD024803

Anchukaitis, K.J., Wilson, R., Briffa, K.R., Buntgen, U., Cook, E.R., D'Arrigo, R., Davi, N., Esper, J., Frank, D., Gunnarson, B.E., Hegerl, G., Helama, S., Klesse, S., Krusic, P.J., Linderholm, H.W., Myglan, V., Osborn, T.J., Zhang, P., Rydval, M., Schneider, L., Schurer, A., Wiles, G., Zorita, E., 2017. Last millennium Northern Hemisphere summer temperatures from tree rings: Part II, spatially resolved reconstructions. Quat. Sci. Rev. 163, 1–22. https://doi.org/10.1016/j.quascirev.2017.02.020

Andrews, T., Forster, P.M., Boucher, O., Bellouin, N., Jones, A., 2010. Precipitation, radiative forcing and global temperature change. Geophys. Res. Lett. 37. https://doi.org/10.1029/2010GL043991

Andronova, N.G., Schlesinger, M.E., 2000. Causes of global temperature changes during the 19th and 20th centuries. Geophys. Res. Lett. 27, 2137–2140. https://doi.org/10.1029/2000GL006109

Armour, K.C., Marshall, J., Scott, J.R., Donohoe, A., Newsom, E.R., 2016. Southern Ocean warming delayed by circumpolar upwelling and equatorward transport. Nat. Geosci. 9, 549–554. https://doi.org/10.1038/ngeo2731

Arneth A. et al., 2019: Climate Change and Land. IPCC special report on climate change, desertification, land degradation, sustainable land management, food security, and greenhouse gas fluxes in terrestrial ecosystems. From https://www.ipcc.ch/srccl-report-

download-page/

Bala, G., Caldeira, K., Nemani, R., 2010. Fast versus slow response in climate change: implications for the global hydrological cycle. Clim. Dyn. 35, 423–434. https://doi.org/10.1007/s00382-009-0583-y

Becker, A., Finger, P., Meyer-Christoffer, A., Rudolf, B., Schamm, K., Schneider, U., Ziese, M., 2013. A description of the global land-surface precipitation data products of the Global Precipitation Climatology Centre with sample applications including centennial (trend) analysis from 1901–present. Earth Syst. Sci. Data 5, 71–99. https://doi.org/10.5194/essd-5-71-2013

Bellomo, K., Murphy, L.N., Cane, M.A., Clement, A.C., Polvani, L.M., 2018. Historical forcings as main drivers of the Atlantic multidecadal variability in the CESM large ensemble. Clim. Dyn. 50, 3687–3698. https://doi.org/10.1007/s00382-017-3834-3

Benestad, R.E., Schmidt, G.A., 2009. Solar trends and global warming. J. Geophys. Res. Atmospheres 114. https://doi.org/10.1029/2008JD011639

Bengtsson, L., Semenov, V.A., Johannessen, O.M., 2004. The Early Twentieth-Century Warming in the Arctic—A Possible Mechanism. J. Clim. 17, 4045–4057. https://doi.org/10.1175/1520-0442(2004)017<4045:TETWIT>2.0.CO;2

Bersch, M., Yashayaev, I., Koltermann, K.P., 2007. Recent changes of the thermohaline circulation in the subpolar North Atlantic. Ocean Dyn. 57, 223–235. https://doi.org/10.1007/s10236-007-0104-7

Biasutti, M., 2013. Forced Sahel rainfall trends in the CMIP5 archive. J. Geophys. Res. Atmospheres 118, 1613–1623. https://doi.org/10.1002/jgrd.50206

Bindoff, N.L., Stott, P.A., AchutaRao, K.M., Allen, M.R., Gillett, N., Gutzler, D., Hansingo, K., Hegerl, G., Hu, Y., Jain, S., Mokhov, I.I., Overland, J., Perlwitz, J., Sebbari, R., Zhang, X., , 2014. Detection and Attribution of Climate Change: from Global to Regional, in: Stocker, TF and Qin, D and Plattner, GK and Tignor, MMB and Allen, SK and Boschung, J and Nauels, A and Xia, Y and Bex, V and Midgley, PM (Ed.), CLIMATE CHANGE 2013: THE PHYSICAL SCIENCE BASIS. pp. 867–952.

Böhm, R., Jones, P.D., Hiebl, J., Frank, D., Brunetti, M., Maugeri, M., 2010. The early instrumental warm-bias: a solution for long central European temperature series 1760–2007. Clim. Change 101, 41–67. https://doi.org/10.1007/s10584-009-9649-4

Bollasina, M.A., Ming, Y., Ramaswamy, V., 2011. Anthropogenic Aerosols and the Weakening of the South Asian Summer Monsoon. Science 334, 502–505. https://doi.org/10.1126/science.1204994

Booth, B.B.B., Dunstone, N.J., Halloran, P.R., Andrews, T., Bellouin, N., 2012. Aerosols implicated as a prime driver of twentieth-century North Atlantic climate variability. Nature 484, 228–232. https://doi.org/10.1038/nature10946

Booth, B.B.B., Harris, G.R., Jones, A., Wilcox, L., Hawcroft, M., Carslaw, K.S., 2018. Comments on "Rethinking the Lower Bound on Aerosol Radiative Forcing." J. Clim. 31, 9407–9412. https://doi.org/10.1175/JCLI-D-17-0369.1

Brohan, P., Compo, G.P., Brönnimann, S., Allan, R.J., Auchmann, R., Brugnara, Y., Sardeshmukh, P.D., Whitaker, J.S., 2016. The 1816 'year without a summer' in an atmospheric reanalysis. Clim. Past Discuss. 1–11. https://doi.org/10.5194/cp-2016-78

Brönnimann, S., 2009. Early twentieth-century warming. Nat. Geosci. 2, 735–736. https://doi.org/10.1038/ngeo670

Brönnimann, S., 2019b. Unlocking pre-1850 instrumental meteorological records: A global inventory. Bull. Am. Meteorol. Soc. (accepted)

Brönnimann, S., Fischer, A.M., Rozanov, E., Poli, P., Compo, G.P., Sardeshmukh, P.D., 2015. Southward shift of the northern tropical belt from 1945 to 1980. Nat. Geosci. 8, 969–974. https://doi.org/10.1038/ngeo2568

Brönnimann, S., Franke, J., Nussbaumer, U., Zumbühl, H.J., Steiner, D., Trachsel, M., Hegerl, G.C., Schurer, A., Worni, M., Malik, A., Flückiger, J., Raible, C.C., 2019a. Volcanoes forced last

phase of Little Ice Age. Nat. Geosci., **12,** 650-656

Cao, L., Bala, G., Caldeira, K., 2012. Climate response to changes in atmospheric carbon dioxide and solar irradiance on the time scale of days to weeks. Environ. Res. Lett. 7, 034015. https://doi.org/10.1088/1748-9326/7/3/034015

Carslaw, K.S., Lee, L.A., Reddington, C.L., Pringle, K.J., Rap, A., Forster, P.M., Mann, G.W., Spracklen, D.V., Woodhouse, M.T., Regayre, L.A., Pierce, J.R., 2013. Large contribution of natural aerosols to uncertainty in indirect forcing. Nature 503, 67–71. https://doi.org/10.1038/nature12674

Chan, D., Huybers, P., 2019. Systematic Differences in Bucket Sea Surface Temperature Measurements among Nations Identified Using a Linear-Mixed-Effect Method. J. Clim. 32, 2569–2589. https://doi.org/10.1175/JCLI-D-18-0562.1

Chang, C.-Y., Chiang, J.C.H., Wehner, M.F., Friedman, A.R., Ruedy, R., 2011. Sulfate aerosol control of Tropical Atlantic climate over the Twentieth Century. J. Clim. 110301125651015. https://doi.org/10.1175/2010JCLI4065.1

Chiang, J.C.H., Friedman, A.R., 2012. Extratropical Cooling, Interhemispheric Thermal Gradients, and Tropical Climate Change. Annu. Rev. Earth Planet. Sci. 40, 383–412. https://doi.org/10.1146/annurev-earth-042711-105545

Chung, E.-S., Timmermann, A., Soden, B.J., Ha, K.-J., Shi, L., John, V.O., 2019. Reconciling opposing Walker circulation trends in observations and model projections. Nat. Clim. Change 9, 405. https://doi.org/10.1038/s41558-019-0446-4

Cole-Dai, J., Ferris, D., Lanciki, A., Savarino, J., Baroni, M., Thiemens, M.H., 2016. Cold decade (AD 1810–1819) caused by Tambora (1815) and another (1809) stratospheric volcanic eruption. Paleoceanography. https://doi.org/10.1029/2009GL040882@10.1002/(ISSN)1944-9186.WAISDIV

Collins, M., Knutti, R., Arblaster, J., Dufresne, J.-L., Fichefet, T., Friedlingstein, P., Gao, X., Gutowski, W.J., Jr., Johns, T., Krinner, G., Shongwe, M., Tebaldi, C., Weaver, A.J., Wehner, 2014. Long-term Climate Change: Projections, Commitments and Irreversibility, in: Stocker, TF and Qin, D and Plattner, GK and Tignor, MMB and Allen, SK and Boschung, J and Nauels, A and Xia, Y and Bex, V and Midgley, PM (Ed.), CLIMATE CHANGE 2013: THE PHYSICAL SCIENCE BASIS. pp. 1029–1136.

Compo, G.P., Whitaker, J.S., Sardeshmukh, P.D., Matsui, N., Allan, R.J., Yin, X., Gleason, B.E., Vose, R.S., Rutledge, G., Bessemoulin, P., Brönnimann, S., Brunet, M., Crouthamel, R.I., Grant, A.N., Groisman, P.Y., Jones, P.D., Kruk, M.C., Kruger, A.C., Marshall, G.J., Maugeri, M., Mok, H.Y., Nordli, Ø., Ross, T.F., Trigo, R.M., Wang, X.L., Woodruff, S.D., Worley, S.J., 2011. The Twentieth Century Reanalysis Project. Q. J. R. Meteorol. Soc. 137, 1–28. https://doi.org/10.1002/qj.776

Cowan, T., Cai, W., 2013. The response of the large-scale ocean circulation to 20th century Asian and non-Asian aerosols. Geophys. Res. Lett. 40, 2761–2767. https://doi.org/10.1002/grl.50587

Cowan, T., Hegerl, G.C., Colfescu, I., Bollasina, M., Purich, A., Boschat, G., 2017. Factors Contributing to Record-Breaking Heat Waves over the Great Plains during the 1930s Dust Bowl. J. Clim. 30, 2437–2461. https://doi.org/10.1175/JCLI-D-16-0436.1

Cox et al. (2018) Emergent constraint on equilibrium climate sensitivity from global temperature variability. Nature 553, 319-322

Cowtan, K., Hausfather, Z., Hawkins, E., Jacobs, P., Mann, M.E., Miller, S.K., Steinman, B.A., Stolpe, M.B., Way, R.G., 2015. Robust comparison of climate models with observations using blended land air and ocean sea surface temperatures. Geophys. Res. Lett. 42, 2015GL064888. https://doi.org/10.1002/2015GL064888

Crowley, T.J., Obrochta, S.P., Liu, J., 2014. Recent global temperature "plateau" in the context of a new proxy reconstruction. Earths Future 2, 281–294. https://doi.org/10.1002/2013EF000216

Czaja, A., Marshall, J., 2001. Observations of atmosphere-ocean coupling in the North Atlantic. Q. J. R. Meteorol. Soc. 127, 1893–1916. https://doi.org/10.1002/qj.49712757603

Dai, A., 2016. Historical and future changes in streamflow and continental runoff: A review. Chapter 2, 17–37.

Dai, A., Qian, T., Trenberth, K.E., Milliman, J.D., 2009. Changes in Continental Freshwater Discharge from 1948 to 2004. J. Clim. 22, 2773–2792. https://doi.org/10.1175/2008JCLI2592.1

Davis, N.A., Davis, S.M., 2018. Reconciling Hadley Cell Expansion Trend Estimates in Reanalyses. Geophys. Res. Lett. 45, 11,439-11,446. https://doi.org/10.1029/2018GL079593

Day, J.J., Hargreaves, J.C., Annan, J.D., Abe-Ouchi, A., 2012. Sources of multi-decadal variability in Arctic sea ice extent. Environ. Res. Lett. 7, 034011. https://doi.org/10.1088/1748-9326/7/3/034011

de Noblet-Ducoudré, N., Boisier, J.-P., Pitman, A., Bonan, G.B., Brovkin, V., Cruz, F., Delire, C., Gayler, V., van den Hurk, B.J.J.M., Lawrence, P.J., van der Molen, M.K., Müller, C., Reick, C.H., Strengers, B.J., Voldoire, A., 2012. Determining Robust Impacts of Land-Use-Induced Land Cover Changes on Surface Climate over North America and Eurasia: Results from the First Set of LUCID Experiments. J. Clim. 25, 3261–3281. https://doi.org/10.1175/JCLI-D-11-00338.1

Delworth, T.L., Dixon, K.W., 2006. Have anthropogenic aerosols delayed a greenhouse gas-induced weakening of the North Atlantic thermohaline circulation? Geophys. Res. Lett. 33. https://doi.org/10.1029/2005GL024980

Delworth, T.L., Knutson, T.R., 2000. Simulation of Early 20th Century Global Warming. Science 287, 2246–2250. https://doi.org/10.1126/science.287.5461.2246

Delworth, T.L., Mann, M.E., 2000. Observed and simulated multidecadal variability in the Northern Hemisphere. Clim. Dyn. 16, 661–676. https://doi.org/10.1007/s003820000075

Deser, C., Hurrell, J.W., Phillips, A.S., 2017. The role of the North Atlantic Oscillation in European climate projections. Clim. Dyn. 49, 3141–3157. https://doi.org/10.1007/s00382-016-3502-z

Dey, R., Lewis, S.C., Abram, N.J., 2019. Investigating observed northwest Australian rainfall trends in Coupled Model Intercomparison Project phase 5 detection and attribution experiments. Int. J. Climatol. 39, 112–127. https://doi.org/10.1002/joc.5788

Donat, M.G., King, A.D., Overpeck, J.T., Alexander, L.V., Durre, I., Karoly, D.J., 2016. Extraordinary heat during the 1930s US Dust Bowl and associated large-scale conditions. Clim. Dyn. 46, 413–426. https://doi.org/10.1007/s00382-015-2590-5

Dong, B., Sutton, R.T., Highwood, E., Wilcox, L., 2014. The Impacts of European and Asian Anthropogenic Sulfur Dioxide Emissions on Sahel Rainfall. J. Clim. 27, 7000–7017. https://doi.org/10.1175/JCLI-D-13-00769.1

Durack, P.J., Wijffels, S.E., Matear, R.J., 2012. Ocean Salinities Reveal Strong Global Water Cycle Intensification During 1950 to 2000. Science 336, 455–458. https://doi.org/10.1126/science.1212222

Eden, C., Greatbatch, R.J., 2003. A Damped Decadal Oscillation in the North Atlantic Climate System. J. Clim. 16, 4043–4060. https://doi.org/10.1175/1520-0442(2003)016<4043:ADDOIT>2.0.CO;2

Eden, C., Jung, T., 2001. North Atlantic Interdecadal Variability: Oceanic Response to the North Atlantic Oscillation (1865–1997). J. Clim. 14, 676–691. https://doi.org/10.1175/1520-0442(2001)014<0676:NAIVOR>2.0.CO;2

Eden, C., Willebrand, J., 2001. Mechanism of Interannual to Decadal Variability of the North Atlantic Circulation. J. Clim. 14, 2266–2280. https://doi.org/10.1175/1520-0442(2001)014<2266:MOITDV>2.0.CO;2

England, M.H., McGregor, S., Spence, P., Meehl, G.A., Timmermann, A., Cai, W., Gupta, A.S., McPhaden, M.J., Purich, A., Santoso, A., 2014. Recent intensification of wind-driven circulation in the Pacific and the ongoing warming hiatus. Nat. Clim. Change 4, 222–227. https://doi.org/10.1038/nclimate2106

Ferguson, C. R., Villarini, G., 2012. Detecting Inhomogeneities in the Twentieth Century Reanalysis over the central United States. J. Geophys. Res., 117, D05123, doi:10.1029/ 2011JD016988.

Flato, G., Marotzke, J., Abiodun, B., Braconnot, P., Chou, S.C., Collins, W.J., Cox, P., Driouech, F., Emori, S., Eyring, V., Forest, C., Gleckler, P., Guilyardi, E., Jakob, C., Kattsov, V., Reason, C., Rummukaines, M., 2013. Evaluation of Climate Models. In: Climate Change 2013: The Physical Science Basis. Contribution of Working Group I to the Fifth Assessment Report of the Intergovernmental Panel on Climate Change, in: Climate Change 2013. Cambridge University Press, pp. 741–866.

Folland, C.K., Boucher, O., Colman, A., Parker, D.E., 2018. Causes of irregularities in trends of global mean surface temperature since the late 19th century. Sci. Adv. 4, eaao5297. https://doi.org/10.1126/sciadv.aao5297

Folland, C.K., Parker, D.E., 1995. Correction of instrumental biases in historical sea surface temperature data. Q. J. R. Meteorol. Soc. 121, 319–367. https://doi.org/10.1002/qj.49712152206

Franke, J., Brönnimann, S., Bhend, J., Brugnara, Y., 2017. A monthly global paleo-reanalysis of the atmosphere from 1600 to 2005 for studying past climatic variations. Sci. Data 4, 170076. https://doi.org/10.1038/sdata.2017.76

Frankignoul, C., Hasselmann, K., 1977. Stochastic climate models, Part II Application to sea-surface temperature anomalies and thermocline variability. Tellus 29, 289–305. https://doi.org/10.3402/tellusa.v29i4.11362

Friedman, A.R., Hegerl, G.C., Schurer, A.P., Lee, S.-Y., W. Kong, Cheng, W., Chiang, J.C.H., in revision. Forced and unforced decadal behavior of the interhemispheric SST contrast during the instrumental period (1881–2012): contextualizing the abrupt shift around 1970. J. Clim.

Friedman, A.R., Reverdin, G., Khodri, M., Gastineau, G., 2017. A new record of Atlantic sea surface salinity from 1896 to 2013 reveals the signatures of climate variability and long-term trends. Geophys. Res. Lett. 2017GL072582. https://doi.org/10.1002/2017GL072582

Fyfe, J.C., Meehl, G.A., England, M.H., Mann, M.E., Santer, B.D., Flato, G.M., Hawkins, E., Gillett, N.P., Xie, S.-P., Kosaka, Y., Swart, N.C., 2016. Making sense of the early-2000s warming slowdown. Nat. Clim. Change 6, 224–228. https://doi.org/10.1038/nclimate2938

García-Herrera, R., Barriopedro, D., Gallego, D., Mellado-Cano, J., Wheeler, D., Wilkinson, C., 2018. Understanding weather and climate of the last 300 years from ships' logbooks. Wiley Interdiscip. Rev. Clim. Change 9, e544. https://doi.org/10.1002/wcc.544

Gedney, N., Cox, P.M., Betts, R.A., Boucher, O., Huntingford, C., Stott, P.A., 2006. Detection of a direct carbon dioxide effect in continental river runoff records. Nature 439, 835. https://doi.org/10.1038/nature04504

Gerten, D., Rost, S., Bloh, W. von, Lucht, W., 2008. Causes of change in 20th century global river discharge. Geophys. Res. Lett. 35. https://doi.org/10.1029/2008GL035258

Gillett, N.P., Arora, V.K., Flato, G.M., Scinocca, J.F., Salzen, K. von, 2012. Improved constraints on 21st-century warming derived using 160 years of temperature observations. Geophys. Res. Lett. 39. https://doi.org/10.1029/2011GL050226

Gillett, N.P., Arora, V.K., Matthews, D., Allen, M.R., 2013. Constraining the Ratio of Global Warming to Cumulative CO2 Emissions Using CMIP5 Simulations. J. Clim. 26, 6844–6858. https://doi.org/10.1175/JCLI-D-12-00476.1

Goodwin, P. , 2018. On the time evolution of climate sensitivity and future warming. Earth's Future, 6, 1336–1348.

Goodwin, P., Katavouta, A., Roussenov, V.M., Foster, G.L., Rohling, E.J. and Williams, R.G., 2018. Pathways to 1.5 and 2 °C warming based on observational and geological constraints. Nature Geoscience 11, 102-107.

Gray, L.J., Beer, J., Geller, M., Haigh, J.D., Lockwood, M., Matthes, K., Cubasch, U., Fleitmann, D., Harrison, G., Hood, L., Luterbacher, J., Meehl, G.A., Shindell, D., van Geel, B., White, W., 2010. Solar influences on climate. Rev. Geophys. 48. https://doi.org/10.1029/2009RG000282

Gray, L.J., Woollings, T.J., Andrews, M., Knight, J., 2016. Eleven-year solar cycle signal in the NAO and Atlantic/European blocking. Q. J. R. Meteorol. Soc. 142, 1890–1903.

https://doi.org/10.1002/qj.2782
Greve, P., Orlowsky, B., Mueller, B., Sheffield, J., Reichstein, M., Seneviratne, S.I., 2014. Global assessment of trends in wetting and drying over land. Nat. Geosci. 7, 716–721. https://doi.org/10.1038/ngeo2247
Guevara-Murua, A., Williams, C.A., Hendy, E.J., Rust, A.C., Cashman, K.V., 2014. Observations of a stratospheric aerosol *veil* from a tropical volcanic eruption in December 1808: is this the *Unknown* ∼1809 eruption? Clim. Past 10, 1707–1722. https://doi.org/10.5194/cp-10-1707-2014
Gulev, S.K., Latif, M., Keenlyside, N., Park, W., Koltermann, K.P., 2013. North Atlantic Ocean control on surface heat flux on multidecadal timescales. Nature 499, 464–467. https://doi.org/10.1038/nature12268
Guo, L., Highwood, E.J., Shaffrey, L.C., Turner, A.G., 2013. The effect of regional changes in anthropogenic aerosols on rainfall of the East Asian Summer Monsoon. Atmospheric Chem. Phys. 13, 1521–1534. https://doi.org/10.5194/acp-13-1521-2013
Guo, L., Turner, A.G., Highwood, E.J., 2015. Impacts of 20th century aerosol emissions on the South Asian monsoon in the CMIP5 models. Atmospheric Chem. Phys. 15, 6367–6378. https://doi.org/10.5194/acp-15-6367-2015
Hannart, A., Ribes, A., Naveau, P., 2014. Optimal fingerprinting under multiple sources of uncertainty. Geophys. Res. Lett. 41, 1261–1268. https://doi.org/10.1002/2013GL058653
Harrington, L.J., Otto, F.E.L., Cowan, T., Hegerl, G.C., 2019. Circulation analogues and uncertainty in the time-evolution of extreme event probabilities: evidence from the 1947 Central European heatwave. Clim. Dyn. https://doi.org/10.1007/s00382-019-04820-2
Harris, I., Jones, P.D., Osborn, T.J., Lister, D.H., 2014. Updated high-resolution grids of monthly climatic observations – the CRU TS3.10 Dataset. Int. J. Climatol. 34, 623–642. https://doi.org/10.1002/joc.3711
Hasselmann, K., 1997. Multi-pattern fingerprint method for detection and attribution of climate change. Clim. Dyn. 13, 601–611. https://doi.org/10.1007/s003820050185
Hasselmann, K., 1979. On the Problem of Multiple Time Scales in Climate Modeling, in: Bach, W., Pankrath, J., Kellogg, W. (Eds.), Developments in Atmospheric Science, Man's Impact on Climate. Elsevier, pp. 43–55. https://doi.org/10.1016/B978-0-444-41766-4.50011-4
Hasselmann, K., 1976. Stochastic climate models Part I. Theory. Tellus 28, 473–485. https://doi.org/10.3402/tellusa.v28i6.11316
Haustein, K., Otto, F.E.L., Venema, V., Jacobs, P., Cowtan, K., Hausfather, Z., Way, R.G., White, B., Subramanian, A., Schurer, A.P., 2019. A limited role for unforced internal variability in 20th century warming. J. Clim. https://doi.org/10.1175/JCLI-D-18-0555.1
Hawkins, E., Ortega, P., Suckling, E., Schurer, A., Hegerl, G., Jones, P., Joshi, M., Osborn, T.J., Masson-Delmotte, V., Mignot, J., Thorne, P., van Oldenborgh, G.J., 2017. ESTIMATING CHANGES IN GLOBAL TEMPERATURE SINCE THE PREINDUSTRIAL PERIOD. Bull. Am. Meteorol. Soc. 98, 1841–1856. https://doi.org/10.1175/BAMS-D-16-0007.1
Hegerl, G., Luterbacher, J., Gonzalez-Rouco, F., Tett, S.F.B., Crowley, T., Xoplaki, E., 2011. Influence of human and natural forcing on European seasonal temperatures. Nat. Geosci. 4, 99–103. https://doi.org/10.1038/NGEO1057
Hegerl, G., vonStorch, H., Hasselmann, K., Santer, B., Cubasch, U., Jones, P., 1996. Detecting greenhouse-gas-induced climate change with an optimal fingerprint method. J. Clim. 9, 2281–2306. https://doi.org/10.1175/1520-0442(1996)009<2281:DGGICC>2.0.CO;2
Hegerl, G.C., Black, E., Allan, R.P., Ingram, W.J., Polson, D., Trenberth, K.E., Chadwick, R.S., Arkin, P.A., Sarojini, B.B., Becker, A., Dai, A., Durack, P.J., Easterling, D., Fowler, H.J., Kendon, E.J., Huffman, G.J., Liu, C., Marsh, R., New, M., Osborn, T.J., Skliris, N., Stott, P.A., Vidale, P.-L., Wijffels, S.E., Wilcox, L.J., Willett, K.M., Zhang, X., 2015. CHALLENGES IN QUANTIFYING CHANGES IN THE GLOBAL WATER CYCLE. Bull. Am. Meteorol. Soc. 96, 1097–1115. https://doi.org/10.1175/BAMS-D-13-00212.1

Hegerl, G.C., Bronnimann, S., Schurer, A., Cowan, T., 2018. The early 20th century warming: Anomalies, causes, and consequences. WILEY Interdiscip. Rev.-Clim. CHANGE 9. https://doi.org/10.1002/wcc.522

Held, I.M., Delworth, T.L., Lu, J., Findell, K. u, Knutson, T.R., 2005. Simulation of Sahel drought in the 20th and 21st centuries. Proc. Natl. Acad. Sci. 102, 17891–17896.

Hoesly, R.M., Smith, S.J., Feng, L., Klimont, Z., Janssens-Maenhout, G., Pitkanen, T., Seibert, J.J., Vu, L., Andres, R.J., Bolt, R.M., Bond, T.C., Dawidowski, L., Kholod, N., Kurokawa, J., Li, M., Liu, L., Lu, Z., Moura, M.C.P., O'Rourke, P.R., Zhang, Q., 2018. Historical (1750–2014) anthropogenic emissions of reactive gases and aerosols from the Community Emissions Data System (CEDS). Geosci. Model Dev. 11, 369–408. https://doi.org/10.5194/gmd-11-369-2018

Hu, S., Fedorov, A.V., 2017. The extreme El Niño of 2015–2016 and the end of global warming hiatus. Geophys. Res. Lett. 44, 3816–3824. https://doi.org/10.1002/2017GL072908

Huang, B., Thorne, P.W., Banzon, V.F., Boyer, T., Chepurin, G., Lawrimore, J.H., Menne, M.J., Smith, T.M., Vose, R.S., Zhang, H.-M., 2017. Extended Reconstructed Sea Surface Temperature, Version 5 (ERSSTv5): Upgrades, Validations, and Intercomparisons. J. Clim. 30, 8179–8205. https://doi.org/10.1175/JCLI-D-16-0836.1

Huffman, G.J., Adler, R.F., Bolvin, D.T., Gu, G., 2009. Improving the global precipitation record: GPCP Version 2.1. Geophys. Res. Lett. 36. https://doi.org/10.1029/2009GL040000

Hulme, M., Jones, P., 1994. Global Climate-Change in the Instrumental Period. Environ. Pollut. 83, 23–36. https://doi.org/10.1016/0269-7491(94)90019-1

Hurrell, J.W., 1995. Decadal Trends in the North Atlantic Oscillation: Regional Temperatures and Precipitation. Science 269, 676–679. https://doi.org/10.1126/science.269.5224.676

Hurrell, J.W., Deser, C., 2009. North Atlantic climate variability: The role of the North Atlantic Oscillation. J. Mar. Syst. 78, 28–41. https://doi.org/10.1016/j.jmarsys.2008.11.026

Hurrell, J.W., Kushnir, Y., Ottersen, G., Visbeck, M.H., 2003. An Overview of the North Atlantic Oscillation, in: The North Atlantic Oscillation: Climate Significance and Environmental Impact, Geophysical Monograph Series. pp. 1–35.

Hurrell, J.W., Van Loon, H., 1997. Decadal Variations in Climate Associated with the North Atlantic Oscillation, in: Diaz, H.F., Beniston, M., Bradley, R.S. (Eds.), Climatic Change at High Elevation Sites. Springer Netherlands, Dordrecht, pp. 69–94. https://doi.org/10.1007/978-94-015-8905-5_4

Hwang, Y.-T., Frierson, D.M.W., Kang, S.M., 2013. Anthropogenic sulfate aerosol and the southward shift of tropical precipitation in the late 20th century. Geophys. Res. Lett. 40, 2845–2850. https://doi.org/10.1002/grl.50502

Ifft, G.N., 1922. The changing arctic. Mon. Weather Rev. 50, 589–589. https://doi.org/10.1175/1520-0493(1922)50<589a:TCA>2.0.CO;2

Iles, C., Hegerl, G., 2017. Role of the North Atlantic Oscillation in decadal temperature trends. Environ. Res. Lett. 12. https://doi.org/10.1088/1748-9326/aa9152

Iles, C.E., Hegerl, G.C., 2015. Systematic change in global patterns of streamflow following volcanic eruptions. Nat. Geosci. 8, 838+. https://doi.org/10.1038/NGEO2545

Iles, C.E., Hegerl, G.C., Schurer, A.P., Zhang, X., 2013. The effect of volcanic eruptions on global precipitation. J. Geophys. Res.-ATMOSPHERES 118, 8770–8786. https://doi.org/10.1002/jgrd.50678

Ineson, S., Scaife, A.A., Knight, J.R., Manners, J.C., Dunstone, N.J., Gray, L.J., Haigh, J.D., 2011. Solar forcing of winter climate variability in the Northern Hemisphere. Nat. Geosci. 4, 753–757. https://doi.org/10.1038/ngeo1282

IPCC, 2018. Summary for Policymakers — Global Warming of 1.5 °C, in: Masson-Delmotte, V., Zhai, P., Pörtner, H.-O., Roberts, D., Skea, J., Shukla, P.R., Pirani, A., Moufouma-Okia, W., Péan, C., Pidcock, R., Connors, S., Matthews, J.B.R., Chen, Y., Zhou, X., Gomis, M.I., Lonnoy, E., Maycock, T., Tignor, M., Waterfield, T. (Eds.), Global Warming of 1.5°C. An IPCC Special Report on the Impacts of Global Warming of 1.5°C above Pre-Industrial Levels and Related

Global Greenhouse Gas Emission Pathways, in the Context of Strengthening the Global Response to the Threat of Climate Change, Sustainable Development, and Efforts to Eradicate Poverty. Geneva, Switzerland, p. 32.

Johannessen, O.M., Bengtsson, L., Miles, M.W., Kuzmina, S.I., Semenov, V.A., Alekseev, G.V., Nagurnyi, A.P., Zakharov, V.F., Bobylev, L.P., Pettersson, L.H., Hasselmann, K., Cattle, H.P., 2004. Arctic climate change: observed and modelled temperature and sea-ice variability. Tellus Dyn. Meteorol. Oceanogr. 56, 328–341. https://doi.org/10.3402/tellusa.v56i4.14418

Jones, G.S., Kennedy, J.J., 2017. Sensitivity of Attribution of Anthropogenic Near-Surface Warming to Observational Uncertainty. J. Clim. 30, 4677–4691. https://doi.org/10.1175/JCLI-D-16-0628.1

Jones, G.S., Stott, P.A., Christidis, N., 2013. Attribution of observed historical near–surface temperature variations to anthropogenic and natural causes using CMIP5 simulations. J. Geophys. Res. Atmospheres 118, 4001–4024. https://doi.org/10.1002/jgrd.50239

Jones, J.M., Gille, S.T., Goosse, H., Abram, N.J., Canziani, P.O., Charman, D.J., Clem, K.R., Crosta, X., de Lavergne, C., Eisenman, I., England, M.H., Fogt, R.L., Frankcombe, L.M., Marshall, G.J., Masson-Delmotte, V., Morrison, A.K., Orsi, A.J., Raphael, M.N., Renwick, J.A., Schneider, D.P., Simpkins, G.R., Steig, E.J., Stenni, B., Swingedouw, D., Vance, T.R., 2016. Assessing recent trends in high-latitude Southern Hemisphere surface climate. Nat. Clim. Change 6, 917–926. https://doi.org/10.1038/nclimate3103

Jones, P.D., Lister, D.H., Osborn, T.J., Harpham, C., Salmon, M., Morice, C.P., 2012. Hemispheric and large-scale land-surface air temperature variations: An extensive revision and an update to 2010. J. Geophys. Res. 117, 29 PP. https://doi.org/201210.1029/2011JD017139

Jungclaus, J.H., Fischer, N., Haak, H., Lohmann, K., Marotzke, J., Matei, D., Mikolajewicz, U., Notz, D., von Storch, J.S., 2013. Characteristics of the ocean simulations in the Max Planck Institute Ocean Model (MPIOM) the ocean component of the MPI-Earth system model. J. Adv. Model. Earth Syst. 5, 422–446. https://doi.org/10.1002/jame.20023

Jungclaus, J.H., Haak, H., Latif, M., Mikolajewicz, U., 2005. Arctic–North Atlantic Interactions and Multidecadal Variability of the Meridional Overturning Circulation. J. Clim. 18, 4013–4031. https://doi.org/10.1175/JCLI3462.1

Kennedy, J.J., 2014. A review of uncertainty in in situ measurements and data sets of sea surface temperature. Rev. Geophys. 52, 1–32. https://doi.org/10.1002/2013RG000434

Kennedy, J.J., Rayner, N.A., Smith, R.O., Parker, D.E., Saunby, M., 2011a. Reassessing biases and other uncertainties in sea surface temperature observations measured in situ since 1850: 1. Measurement and sampling uncertainties. J. Geophys. Res. 116, 13 PP. https://doi.org/201110.1029/2010JD015218

Kennedy, J.J., Rayner, N.A., Smith, R.O., Parker, D.E., Saunby, M., 2011b. Reassessing biases and other uncertainties in sea surface temperature observations measured in situ since 1850: 2. Biases and homogenization. J. Geophys. Res. 116, 22 PP. https://doi.org/201110.1029/2010JD015220

Kent, E.C., Kennedy, J.J., Smith, T.M., Hirahara, S., Huang, B., Kaplan, A., Parker, D.E., Atkinson, C.P., Berry, D.I., Carella, G., Fukuda, Y., Ishii, M., Jones, P.D., Lindgren, F., Merchant, C.J., Morak-Bozzo, S., Rayner, N.A., Venema, V., Yasui, S., Zhang, H.-M., 2016. A Call for New Approaches to Quantifying Biases in Observations of Sea Surface Temperature. Bull. Am. Meteorol. Soc. 98, 1601–1616. https://doi.org/10.1175/BAMS-D-15-00251.1

Kenyon, J., Hegerl, G.C., 2008. Influence of modes of climate variability on global temperature extremes. J. Clim. 21, 3872–3889. https://doi.org/10.1175/2008JCLI2125.1

Khodri, M., Izumo, T., Vialard, J., Janicot, S., Cassou, C., Lengaigne, M., Mignot, J., Gastineau, G., Guilyardi, E., Lebas, N., Robock, A., McPhaden, M.J., 2017. Tropical explosive volcanic eruptions can trigger El Niño by cooling tropical Africa. Nat. Commun. 8, 778. https://doi.org/10.1038/s41467-017-00755-6

Knight, J.R., 2009. The Atlantic Multidecadal Oscillation Inferred from the Forced Climate Response in Coupled General Circulation Models. J. Clim. 22, 1610–1625.

https://doi.org/10.1175/2008JCLI2628.1

Knudsen, M.F., Jacobsen, B.H., Seidenkrantz, M.-S., Olsen, J., 2014. Evidence for external forcing of the Atlantic Multidecadal Oscillation since termination of the Little Ice Age. Nat. Commun. 5, 3323. https://doi.org/10.1038/ncomms4323

Knutson, T.R., Zeng, F., Wittenberg, A.T., 2013. Multimodel Assessment of Regional Surface Temperature Trends: CMIP3 and CMIP5 Twentieth-Century Simulations. J. Clim. 26, 8709–8743. https://doi.org/10.1175/JCLI-D-12-00567.1

Knutti, R., Allen, M.R., Friedlingstein, P., Gregory, J.M., Hegerl, G.C., Meehl, G.A., Meinshausen, M., Murphy, J.M., Plattner, G.-K., Raper, S.C.B., Stocker, T.F., Stott, P.A., Teng, H., Wigley, T.M.L., 2008. A review of uncertainties in global temperature projections over the twenty-first century. J. Clim. 21, 2651–2663. https://doi.org/10.1175/2007JCLI2119.1

Koch, A., Brierley, C., Maslin, M.M., Lewis, S.L., 2019. Earth system impacts of the European arrival and Great Dying in the Americas after 1492. Quat. Sci. Rev. 207, 13–36. https://doi.org/10.1016/j.quascirev.2018.12.004

Kosaka, Y., Xie, S.-P., 2013. Recent global-warming hiatus tied to equatorial Pacific surface cooling. Nature 501, 403–407. https://doi.org/10.1038/nature12534

Kretzschmar, J., Salzmann, M., Mülmenstädt, J., Boucher, O., Quaas, J., 2017. Comment on "Rethinking the Lower Bound on Aerosol Radiative Forcing." J. Clim. 30, 6579–6584. https://doi.org/10.1175/JCLI-D-16-0668.1

Krueger, O., Schenk, F., Feser, F., Weisse, R., 2012. Inconsistencies between Long-Term Trends in Storminess Derived from the 20CR Reanalysis and Observations. J. Clim. 26, 868–874. https://doi.org/10.1175/JCLI-D-12-00309.1

Laloyaux, P., Boisseson, E. de, Balmaseda, M., Bidlot, J.-R., Brönnimann, S., Buizza, R., Dalhgren, P., Dee, D., Haimberger, L., Hersbach, H., Kosaka, Y., Martin, M., Poli, P., Rayner, N., Rustemeier, E., Schepers, D., 2018. CERA-20C: A Coupled Reanalysis of the Twentieth Century. J. Adv. Model. Earth Syst. 10, 1172–1195. https://doi.org/10.1029/2018MS001273

Lambert, F.H., Allen, M.R., 2009. Are Changes in Global Precipitation Constrained by the Tropospheric Energy Budget? J. Clim. 22, 499–517. https://doi.org/10.1175/2008JCLI2135.1

Lawrence, D.M., Hurtt, G.C., Arneth, A., Brovkin, V., Calvin, K.V., Jones, A.D., Jones, C.D., Lawrence, P.J., Noblet-Ducoudré, N. de, Pongratz, J., Seneviratne, S.I., Shevliakova, E., 2016. The Land Use Model Intercomparison Project (LUMIP) contribution to CMIP6: rationale and experimental design. Geosci. Model Dev. 9, 2973–2998. https://doi.org/10.5194/gmd-9-2973-2016

Lean, J.L., 2018. Estimating Solar Irradiance Since 850 CE. Earth Space Sci. 5, 133–149. https://doi.org/10.1002/2017EA000357

Lehner, F., Deser, C., Terray, L., 2017. Toward a New Estimate of "Time of Emergence" of Anthropogenic Warming: Insights from Dynamical Adjustment and a Large Initial-Condition Model Ensemble. J. Clim. 30, 7739–7756. https://doi.org/10.1175/JCLI-D-16-0792.1

Lehner, F., Schurer, A.P., Hegerl, G.C., Deser, C., Froelicher, T.L., 2016. The importance of ENSO phase during volcanic eruptions for detection and attribution. Geophys. Res. Lett. 43, 2851–2858. https://doi.org/10.1002/2016GL067935

Lewandowsky, S., Risbey, J.S., Oreskes, N., 2016. The "pause" in global warming: Turning a routine fluctuation into a problem for science. Bull. Am. Meteorol. Soc. 97, 723–733.

Li, Z., Lau, W.K.-M., Ramanathan, V., Wu, G., Ding, Y., Manoj, M.G., Liu, J., Qian, Y., Li, J., Zhou, T., Fan, J., Rosenfeld, D., Ming, Y., Wang, Y., Huang, J., Wang, B., Xu, X., Lee, S.-S., Cribb, M., Zhang, F., Yang, X., Zhao, C., Takemura, T., Wang, K., Xia, X., Yin, Y., Zhang, H., Guo, J., Zhai, P.M., Sugimoto, N., Babu, S.S., Brasseur, G.P., 2016. Aerosol and monsoon climate interactions over Asia. Rev. Geophys. 54, 866–929. https://doi.org/10.1002/2015RG000500

Lockwood, M., Harrison, R.G., Woollings, T., Solanki, S.K., 2010. Are cold winters in Europe associated with low solar activity? Environ. Res. Lett. 5, 024001. https://doi.org/10.1088/1748-9326/5/2/024001

Luterbacher, J., Dietrich, D., Xoplaki, E., Grosjean, M., Wanner, H., 2004. European Seasonal and Annual Temperature Variability, Trends, and Extremes Since 1500. Science 303, 1499–1503. https://doi.org/10.1126/science.1093877

Makowski, K., Wild, M., Ohmura, A., 2008. Diurnal temperature range over Europe between 1950 and 2005. Atmospheric Chem. Phys. 8, 6483–6498. https://doi.org/10.5194/acp-8-6483-2008

Manley, G., 1974. Central England temperatures: Monthly means 1659 to 1973. Q. J. R. Meteorol. Soc. 100, 389–405. https://doi.org/10.1002/qj.49710042511

Marvel, K., Cook, B.I., Bonfils, C.J.W., Durack, P.J., Smerdon, J.E., Williams, A.P., 2019. Twentieth-century hydroclimate changes consistent with human influence. Nature 569, 59. https://doi.org/10.1038/s41586-019-1149-8

Masson-Delmotte, V., Schulz, M., Abe-Ouchi, A., Beer, J., Ganopolski, A., Gonzalez Rouco, J.F., Jansen, E., Lambeck, K., Luterbacher, J., Naish, T., Osborn, T., Otto-Bliesner, B., Quinn, T., Ramesh, R., Rojas, M., Shao, X., Timmermann, A., 2013. Information from paleoclimate archives, in: Stocker, T.F., Qin, D., Plattner, G.-K., Tignor, M.M.B., Allen, S.K., Boschung, J., Nauels, A., Xia, Y., Bex, V., Midgley, P.M. (Eds.), Climate Change 2013: The Physical Science Basis. Cambridge University Press, Cambridge, pp. 383–464.

Maugeri, M., Buffoni, L., Chlistovsky, F., 2002. Daily Milan temperature and pressure series (1763-1998): History of the observations and data and metadata recovery. Clim. Change Dordr. 53, 101–117. http://dx.doi.org/10.1023/A:1014970825579

Medhaug, I., Stolpe, M.B., Fischer, E.M., Knutti, R., 2017. Reconciling controversies about the 'global warming hiatus.' Nature 545, 41–47. https://doi.org/10.1038/nature22315

Meehl, G.A., Arblaster, J.M., Matthes, K., Sassi, F., Loon, H. van, 2009. Amplifying the Pacific Climate System Response to a Small 11-Year Solar Cycle Forcing. Science 325, 1114–1118. https://doi.org/10.1126/science.1172872

Menary, M.B., Roberts, C.D., Palmer, M.D., Halloran, P.R., Jackson, L., Wood, R.A., Müller, W.A., Matei, D., Lee, S.-K., 2013. Mechanisms of aerosol-forced AMOC variability in a state of the art climate model. J. Geophys. Res. Oceans 118, 2087–2096. https://doi.org/10.1002/jgrc.20178

Min, S.-K., Zhang, X., Zwiers, F., 2008. Human-Induced Arctic Moistening. Science 320, 518–520. https://doi.org/10.1126/science.1153468

Min, S.-K., Zhang, X., Zwiers, F.W., Hegerl, G.C., 2011. Human contribution to more-intense precipitation extremes. NATURE 470, 378–381. https://doi.org/10.1038/nature09763

Moberg, A., Bergström, H., Krigsman, J.R., Svanered, O., 2002. Daily Air Temperature and Pressure Series for Stockholm (1756–1998), in: Camuffo, D., Jones, P. (Eds.), Improved Understanding of Past Climatic Variability from Early Daily European Instrumental Sources. Springer Netherlands, Dordrecht, pp. 171–212. https://doi.org/10.1007/978-94-010-0371-1_7

Moberg, A., Alexandersson, H., Bergström, H., Jones, P.D., 2003. Were Southern Swedish Summer temperatures before 1860 as warm as measured? Int. J. Climatol. 23, 1495-1521.

Morice, C.P., Kennedy, J.J., Rayner, N.A., Jones, P.D., 2012. Quantifying uncertainties in global and regional temperature change using an ensemble of observational estimates: The HadCRUT4 data set. J. Geophys. Res. Atmospheres 1984–2012 117.

Mueller, B.L., Gillett, N.P., Monahan, A.H., Zwiers, F.W., Mueller, B.L., Gillett, N.P., Monahan, A.H., Zwiers, F.W., 2018. Attribution of Arctic Sea Ice Decline from 1953 to 2012 to Influences from Natural, Greenhouse Gas, and Anthropogenic Aerosol Forcing. J. Clim. https://doi.org/10.1175/JCLI-D-17-0552.1

Müller, W.A., Matei, D., Bersch, M., Jungclaus, J.H., Haak, H., Lohmann, K., Compo, G.P., Sardeshmukh, P.D., Marotzke, J., 2015. A twentieth-century reanalysis forced ocean model to reconstruct the North Atlantic climate variation during the 1920s. Clim. Dyn. 44, 1935–1955. https://doi.org/10.1007/s00382-014-2267-5

Murphy, L.N., Bellomo, K., Cane, M., Clement, A., 2017. The role of historical forcings in simulating

the observed Atlantic multidecadal oscillation. Geophys. Res. Lett. 2016GL071337. https://doi.org/10.1002/2016GL071337

Myhre, G., Shindell, D., Bréon, F.M., Collins, W., Fuglestvedt, J., Huang, J., Koch, D., Lamarque, J.F., Lee, D., Mendoza, B., 2013. Anthropogenic and natural radiative forcing. Climate change 2013: The physical science basis. Contribution of Working Group I to the Fifth Assessment Report of the Intergovernmental Panel on Climate Change, 659–740. Cambridge: Cambridge University Press.

Naylor, S., 2019. Thermometer screens and the geographies of uniformity in nineteenth-century meteorology. Notes Rec. R. Soc. J. Hist. Sci. 73, 203–221. https://doi.org/10.1098/rsnr.2018.0037

Neukom, R., Barboza, L.A., Erb, M.P., Shi, F., Emile-Geay, J., Evans, M.N., Franke, J., Kaufman, D., Lücke, L., Rehfeld, K., Schurer, A., Valler, V., Zhu, F., Brönnimann, S., Hakim, G.J., Henley, B.J., Ljungqvist, F.C., McKay, N., von Gunten, L., 2019. Global multi-decadal temperature variability over the Common Era. Nat. Geosci., **12,** 643-649.

Nguyen, H., Evans, A., Lucas, C., Smith, I., Timbal, B., 2012. The Hadley Circulation in Reanalyses: Climatology, Variability, and Change. J. Clim. 26, 3357–3376. https://doi.org/10.1175/JCLI-D-12-00224.1

O'Gorman, P.A., 2012. Sensitivity of tropical precipitation extremes to climate change. Nat. Geosci. 5, 697–700. https://doi.org/10.1038/ngeo1568

O'Reilly, C.H., Heatley, J., MacLeod, D., Weisheimer, A., Palmer, T.N., Schaller, N., Woollings, T., 2017. Variability in seasonal forecast skill of Northern Hemisphere winters over the twentieth century. Geophys. Res. Lett. 44, 5729–5738. https://doi.org/10.1002/2017GL073736

Otterå, O.H., Bentsen, M., Drange, H., Suo, L., 2010. External forcing as a metronome for Atlantic multidecadal variability. Nat. Geosci. 3, 688–694. https://doi.org/10.1038/ngeo955

PAGES 2k Consortium, Ahmed, M., Anchukaitis, K.J., Asrat, A., Borgaonkar, H.P., Braida, M., Buckley, B.M., Büntgen, U., Chase, B.M., Christie, D.A., Cook, E.R., Curran, M.A.J., Diaz, H.F., Esper, J., Fan, Z.-X., Gaire, N.P., Ge, Q., Gergis, J., González-Rouco, J.F., Goosse, H., Grab, S.W., Graham, N., Graham, R., Grosjean, M., Hanhijärvi, S.T., Kaufman, D.S., Kiefer, T., Kimura, K., Korhola, A.A., Krusic, P.J., Lara, A., Lézine, A.-M., Ljungqvist, F.C., Lorrey, A.M., Luterbacher, J., Masson-Delmotte, V., McCarroll, D., McConnell, J.R., McKay, N.P., Morales, M.S., Moy, A.D., Mulvaney, R., Mundo, I.A., Nakatsuka, T., Nash, D.J., Neukom, R., Nicholson, S.E., Oerter, H., Palmer, J.G., Phipps, S.J., Prieto, M.R., Rivera, A., Sano, M., Severi, M., Shanahan, T.M., Shao, X., Shi, F., Sigl, M., Smerdon, J.E., Solomina, O.N., Steig, E.J., Stenni, B., Thamban, M., Trouet, V., Turney, C.S.M., Umer, M., van Ommen, T., Verschuren, D., Viau, A.E., Villalba, R., Vinther, B.M., von Gunten, L., Wagner, S., Wahl, E.R., Wanner, H., Werner, J.P., White, J.W.C., Yasue, K., Zorita, E., 2013. Continental-scale temperature variability during the past two millennia. Nat. Geosci. 6, 339-346.

PAGES 2k-PMIP3 group, 2015. Continental-scale temperature variability in PMIP3 simulations and PAGES 2k regional temperature reconstructions over the past millennium. Clim Past 11, 1673–1699. https://doi.org/10.5194/cp-11-1673-2015

Parker, D.E., Legg, T.P., Folland, C.K., 1992. A new daily central England temperature series, 1772–1991. Int. J. Climatol. 12, 317–342. https://doi.org/10.1002/joc.3370120402

Piao, S., Friedlingstein, P., Ciais, P., Noblet-Ducoudré, N. de, Labat, D., Zaehle, S., 2007. Changes in climate and land use have a larger direct impact than rising CO2 on global river runoff trends. Proc. Natl. Acad. Sci. 104, 15242–15247. https://doi.org/10.1073/pnas.0707213104

Pitman, A.J., Noblet-Ducoudré, N. de, Cruz, F.T., Davin, E.L., Bonan, G.B., Brovkin, V., Claussen, M., Delire, C., Ganzeveld, L., Gayler, V., Hurk, B.J.J.M. van den, Lawrence, P.J., Molen, M.K. van der, Müller, C., Reick, C.H., Seneviratne, S.I., Strengers, B.J., Voldoire, A., 2009. Uncertainties in climate responses to past land cover change: First results from the LUCID intercomparison study. Geophys. Res. Lett. 36. https://doi.org/10.1029/2009GL039076

Poli, P., Hersbach, H., Dee, D.P., Berrisford, P., Simmons, A.J., Vitart, F., Laloyaux, P., Tan, D.G.H., Peubey, C., Thépaut, J.-N., Trémolet, Y., Hólm, E.V., Bonavita, M., Isaksen, L., Fisher, M., 2016. ERA-20C: An Atmospheric Reanalysis of the Twentieth Century. J. Clim. 29, 4083–4097. https://doi.org/10.1175/JCLI-D-15-0556.1

Polson, D., Bollasina, M., Hegerl, G.C., Wilcox, L.J., 2014. Decreased monsoon precipitation in the Northern Hemisphere due to anthropogenic aerosols. Geophys. Res. Lett. 41, 6023–6029. https://doi.org/10.1002/2014GL060811

Polson, D., Hegerl, G.C., 2017. Strengthening contrast between precipitation in tropical wet and dry regions. Geophys. Res. Lett. 44, 365–373. https://doi.org/10.1002/2016GL071194

Polson, D., Hegerl, G.C., Solomon, S., 2016. Precipitation sensitivity to warming estimated from long island records. Environ. Res. Lett. 11. https://doi.org/10.1088/1748-9326/11/7/074024

Polson, D., Hegerl, G.C., Zhang, X., Osborn, T.J., 2013. Causes of Robust Seasonal Land Precipitation Changes. J. Clim. 26, 6679–6697. https://doi.org/10.1175/JCLI-D-12-00474.1

Polvani, L.M., Banerjee, A., Schmidt, A., 2019. Northern Hemisphere continental winter warming following the 1991 Mt. Pinatubo eruption: reconciling models and observations. Atmospheric Chem. Phys. 19, 6351–6366. https://doi.org/10.5194/acp-19-6351-2019

Polyakov, I.V., Alexeev, V.A., Bhatt, U.S., Polyakova, E.I., Zhang, X., 2010. North Atlantic warming: patterns of long-term trend and multidecadal variability. Clim. Dyn. 34, 439–457. https://doi.org/10.1007/s00382-008-0522-3

Power, S., Casey, T., Folland, C., Colman, A., Mehta, V., 1999. Inter-decadal modulation of the impact of ENSO on Australia. Clim. Dyn. 15, 319–324. https://doi.org/10.1007/s003820050284

Raible, C.C., Brönnimann, S., Auchmann, R., Brohan, P., Frölicher, T.L., Graf, H.-F., Jones, P., Luterbacher, J., Muthers, S., Neukom, R., Robock, A., Self, S., Sudrajat, A., Timmreck, C., Wegmann, M., 2016. Tambora 1815 as a test case for high impact volcanic eruptions: Earth system effects. Wiley Interdiscip. Rev. Clim. Change 7, 569–589. https://doi.org/10.1002/wcc.407

Ribes, A., Planton, S., Terray, L., 2013. Application of regularised optimal fingerprinting to attribution. Part I: method, properties and idealised analysis. Clim. Dyn. 41, 2817–2836. https://doi.org/10.1007/s00382-013-1735-7

Ribes, A., Terray, L., 2013. Application of regularised optimal fingerprinting to attribution. Part II: application to global near-surface temperature. Clim. Dyn. 41, 2837–2853. https://doi.org/10.1007/s00382-013-1736-6

Ribes, A., Zwiers, F.W., Azaïs, J.-M., Naveau, P., 2017. A new statistical approach to climate change detection and attribution. Clim. Dyn. 48, 367–386. https://doi.org/10.1007/s00382-016-3079-6

Richardson T.B. et al., 2018. Drivers of Precipitation Change: An Energetic Understanding. J. Climate 31., 9641-9657.

Roberts, C.D., Palmer, M.D., McNeall, D., Collins, M., 2015. Quantifying the likelihood of a continued hiatus in global warming. Nat. Clim. Change 5, 337–342. https://doi.org/10.1038/nclimate2531

Robock, A., 2000. Volcanic eruptions and climate. Rev. Geophys. 38, 191–219. https://doi.org/10.1029/1998RG000054

Rotstayn, L., Lohmann, U., 2002. Tropical rainfall trends and the indirect aerosol effect. J. Clim. 15, 2103–2116.

Rotstayn, L.D., Jeffrey, S.J., Collier, M.A., Dravitzki, S.M., Hirst, A.C., Syktus, J.I., Wong, K.K., 2012. Aerosol- and greenhouse gas-induced changes in summer rainfall and circulation in the Australasian region: a study using single-forcing climate simulations. Atmospheric Chem. Phys. 12, 6377–6404. https://doi.org/10.5194/acp-12-6377-2012

Rousseau, D., 2015. Variabilité des températures mensuelles à Paris de 1658 à 2014, in: XXVIIIe Colloque de l'Association Internationale de Climatologie. Liège, pp. 597–602.

Santer, B., Mears, C., Wentz, F., Taylor, K., Gleckler, P., Wigley, T., Barnett, T., Boyle, J., Brüggemann,

W., Gillett, N., Klein, S., Meehl, G., Nozawa, T., Pierce, D., Stott, P., Washington, W., WEHNER, M., 2007. Identification of human-induced changes in atmospheric moisture content. Proc. Natl. Acad. Sci. U. S. OF 104, 15248–15253. https://doi.org/10.1073/pnas.0702872104

Sarojini, B.B., Stott, P.A., Black, E., Polson, D., 2012. Fingerprints of changes in annual and seasonal precipitation from CMIP5 models over land and ocean. Geophys. Res. Lett. 39. https://doi.org/10.1029/2012GL053373

Scaife, A.A., Ineson, S., Knight, J.R., Gray, L., Kodera, K., Smith, D.M., 2013. A mechanism for lagged North Atlantic climate response to solar variability. Geophys. Res. Lett. 40, 434–439. https://doi.org/10.1002/grl.50099

Schmidt, G.A., Jungclaus, J.H., Ammann, C.M., Bard, E., Braconnot, P., Crowley, T.J., Delaygue, G., Joos, F., Krivova, N.A., Muscheler, R., Otto-Bliesner, B.L., Pongratz, J., Shindell, D.T., Solanki, S.K., Steinhilber, F., Vieira, L.E.A., 2012. Climate forcing reconstructions for use in PMIP simulations of the Last Millennium (v1.1). Geosci. Model Dev. 5, 185–191. https://doi.org/10.5194/gmd-5-185-2012

Schmitt, R., 2008. Salinity and the Global Water Cycle. Oceanography 21, 12–19. https://doi.org/10.5670/oceanog.2008.63

Schurer, A., Hegerl, G., Ribes, A., Polson, D., Morice, C., Tett, S., 2018. Estimating the Transient Climate Response from Observed Warming. J. Clim. 31, 8645–8663. https://doi.org/10.1175/JCLI-D-17-0717.1

Schurer, A.P., Hegerl, G., Luterbacher, J., Brönnimann, S., Cowan, T., Tett, S. F. B., Zanchettin, D., Timmreck, C., 2019. Disentangling the causes of the 1816 European year without a summer. Environ. Res. Lett. In press.

Schurer, A.P., Hegerl, G.C., Mann, M.E., Tett, S.F.B., Phipps, S.J., 2013. Separating Forced from Chaotic Climate Variability over the Past Millennium. J. Clim. 26, 6954–6973. https://doi.org/10.1175/JCLI-D-12-00826.1

Schurer, A.P., Hegerl, G.C., Obrochta, S.P., 2015. Determining the likelihood of pauses and surges in global warming. Geophys. Res. Lett. 42, 5974–5982. https://doi.org/10.1002/2015GL064458

Schurer, A.P., Mann, M.E., Hawkins, E., Tett, S.F.B., Hegerl, G.C., 2017. Importance of the pre-industrial baseline for likelihood of exceeding Paris goals. Nat. Clim. CHANGE 7, 563–567. https://doi.org/10.1038/NCLIMATE3345

Schurer, A.P., Tett, S.F.B., Hegerl, G.C., 2014. Small influence of solar variability on climate over the past millennium. Nat. Geosci. 7, 104–108. https://doi.org/10.1038/NGEO2040

Shepherd, T.G., 2014. Atmospheric circulation as a source of uncertainty in climate change projections. Nat. Geosci. 7, 703–708. https://doi.org/10.1038/ngeo2253

Shindell, D., Schulz, M., Ming, Y., Takemura, T., Faluvegi, G., Ramaswamy, V., 2010. Spatial scales of climate response to inhomogeneous radiative forcing. J. Geophys. Res. Atmospheres 115. https://doi.org/10.1029/2010JD014108

Shindell, D.T., Faluvegi, G., Rotstayn, L., Milly, G., 2015. Spatial patterns of radiative forcing and surface temperature response. J. Geophys. Res. Atmospheres 120, 5385–5403. https://doi.org/10.1002/2014JD022752

Shiogama, H., Stone, D.A., Nagashima, T., Nozawa, T., Emori, S., 2013. On the linear additivity of climate forcing-response relationships at global and continental scales. Int. J. Climatol. 33, 2542–2550. https://doi.org/10.1002/joc.3607

Skliris, N., Marsh, R., Josey, S.A., Good, S.A., Liu, C., Allan, R.P., 2014. Salinity changes in the World Ocean since 1950 in relation to changing surface freshwater fluxes. Clim. Dyn. 43, 709–736. https://doi.org/10.1007/s00382-014-2131-7

Staten, P.W., Lu, J., Grise, K.M., Davis, S.M., Birner, T., 2018. Re-examining tropical expansion. Nat. Clim. Change 8, 768. https://doi.org/10.1038/s41558-018-0246-2

Steiger, N.J., Smerdon, J.E., Cook, E.R., Cook, B.I., 2018. A reconstruction of global hydroclimate and dynamical variables over the Common Era. Sci. Data 5, 180086.

https://doi.org/10.1038/sdata.2018.86
Stevens, B., 2015. Rethinking the Lower Bound on Aerosol Radiative Forcing. J. Clim. 28, 4794–4819. https://doi.org/10.1175/JCLI-D-14-00656.1
Stevenson, T.C., 1864. New description of box for holding thermometers. J Scott. Meteorol Soc 1, 122.
Stott, P. A., Kettleborough, and J. A., 2002. Origins and estimates of uncertainty in predictions of twenty-first century temperature rise. Nature, 416, 723–726.
Stott, P.A., Jones, G. S., Mitchell, J.F.NB., 2003. Do models underestimate the solar contribution to recent climate change? J. Climate 16, 4079-4093 Geophys. Res. Lett. 30. https://doi.org/10.1175/1520-0442(2003)016%3C4079:DMUTSC%3E2.0.CO;2
Stott, P.A., Christidis, N., Herring, S.C., Hoell, A., Kossin, J.P., Schreck, C.J., 2018. Future Challenges in Event Attribution Methodologies. Bull. Am. Meteorol. Soc. 99, S155–S157. https://doi.org/10.1175/BAMS-D-17-0285.1
Stott, P.A., Christidis, N., Otto, F.E.L., Sun, Y., Vanderlinden, J.-P., Oldenborgh, G.J. van, Vautard, R., Storch, H. von, Walton, P., Yiou, P., Zwiers, F.W., 2016. Attribution of extreme weather and climate-related events. Wiley Interdiscip. Rev. Clim. Change 7, 23–41. https://doi.org/10.1002/wcc.380
Sutton, R., Suckling, E., Hawkins, E., 2015. What does global mean temperature tell us about local climate? Philos. Trans. R. Soc. Math. Phys. Eng. Sci. 373, 20140426. https://doi.org/10.1098/rsta.2014.0426
Swingedouw, D., Mignot, J., Ortega, P., Khodri, M., Menegoz, M., Cassou, C., Hanquiez, V., 2017. Impact of explosive volcanic eruptions on the main climate variability modes. Glob. Planet. Change 150, 24–45. https://doi.org/10.1016/j.gloplacha.2017.01.006
Tandon, N.F., Kushner, P.J., 2015. Does External Forcing Interfere with the AMOC's Influence on North Atlantic Sea Surface Temperature? J. Clim. 28, 6309–6323. https://doi.org/10.1175/JCLI-D-14-00664.1
Tardif, R., Hakim, G.J., Perkins, W.A., Horlick, K.A., Erb, M.P., Emile-Geay, J., Anderson, D.M., Steig, E.J., Noone, D., 2019. Last Millennium Reanalysis with an expanded proxy database and seasonal proxy modeling. Clim. Past 15, 1251–1273. https://doi.org/10.5194/cp-15-1251-2019
Terray, L., Corre, L., Cravatte, S., Delcroix, T., Reverdin, G., Ribes, A., 2012. Near-Surface Salinity as Nature's Rain Gauge to Detect Human Influence on the Tropical Water Cycle. J. Clim. 25, 958–977. https://doi.org/10.1175/JCLI-D-10-05025.1
Tett, S.F.B., Stott, P.A., Allen, M.R., Ingram, W.J., Mitchell, J.F.B., 1999. Causes of twentieth-century temperature change near the Earth's surface. Nature 399, 569. https://doi.org/10.1038/21164
Thompson, D.W.J., Kennedy, J.J., Wallace, J.M., Jones, P.D., 2008. A large discontinuity in the mid-twentieth century in observed global-mean surface temperature. Nature 453, 646–649. https://doi.org/10.1038/nature06982
Thompson, D.W.J., Wallace, J.M., 2001. Regional Climate Impacts of the Northern Hemisphere Annular Mode. Science 293, 85–89. https://doi.org/10.1126/science.1058958
Ting, M., Kushnir, Y., Seager, R., Li, C., 2009. Forced and Internal Twentieth-Century SST Trends in the North Atlantic. J. Clim. 22, 1469–1481. https://doi.org/10.1175/2008JCLI2561.1
Titchner, H.A., Rayner, N.A., 2014. The Met Office Hadley Centre sea ice and sea surface temperature data set, version 2: 1. Sea ice concentrations: HADISST.2.1.0.0 SEA ICE CONCENTRATIONS. J. Geophys. Res. Atmospheres 119, 2864–2889. https://doi.org/10.1002/2013JD020316
Titchner, H.A., Rayner, N.A., in preparation. A detailed assessment of Arctic sea ice extent observations from 1850 onwards.
Toll, V., Christensen, M., Gassó, S., Bellouin, N., 2017. Volcano and Ship Tracks Indicate Excessive Aerosol-Induced Cloud Water Increases in a Climate Model. Geophys. Res. Lett. 44, 12,492-

12,500. https://doi.org/10.1002/2017GL075280
Undorf, S., Bollasina, M.A., Booth, B.B.B., Hegerl, G.C., 2018a. Contrasting the Effects of the 1850-1975 Increase in Sulphate Aerosols from North America and Europe on the Atlantic in the CESM. Geophys. Res. Lett. 45, 11930–11940. https://doi.org/10.1029/2018GL079970
Undorf, S., Bollasina, M.A., Hegerl, G.C., 2018b. Impacts of the 1900-74 Increase in Anthropogenic Aerosol Emissions from North America and Europe on Eurasian Summer Climate. J. Clim. 31, 8381–8399. https://doi.org/10.1175/JCLI-D-17-0850.1
Undorf, S., Polson, D., Bollasina, M.A., Ming, Y., Schurer, A., Hegerl, G.C., 2018c. Detectable Impact of Local and Remote Anthropogenic Aerosols on the 20th Century Changes of West African and South Asian Monsoon Precipitation. J. Geophys. Res.-ATMOSPHERES 123, 4871–4889. https://doi.org/10.1029/2017JD027711
Vecchi, G.A., Soden, B.J., Wittenberg, A.T., Held, I.M., Leetmaa, A., Harrison, M.J., 2006. Weakening of tropical Pacific atmospheric circulation due to anthropogenic forcing. Nature 441, 73–76. https://doi.org/10.1038/nature04744
Wallace, J.M., Zhang, Y., Renwick, J.A., 1995. Dynamic Contribution to Hemispheric Mean Temperature Trends. Science 270, 780–783. https://doi.org/10.1126/science.270.5237.780
Walsh, J.E., Fetterer, F., Stewart, J.S., Chapman, W.L., 2017. A database for depicting Arctic sea ice variations back to 1850. Geogr. Rev. 107, 89–107. https://doi.org/10.1111/j.1931-0846.2016.12195.x
Wang, H., Xie, S.-P., Liu, Q., 2016. Comparison of Climate Response to Anthropogenic Aerosol versus Greenhouse Gas Forcing: Distinct Patterns. J. Clim. 29, 5175–5188. https://doi.org/10.1175/JCLI-D-16-0106.1
Wang, J., Yang, B., Ljungqvist, F.C., Luterbacher, J., Osborn, T.J., Briffa, K.R., Zorita, E., 2017. Internal and external forcing of multidecadal Atlantic climate variability over the past 1,200 years. Nat. Geosci. 10, 512–517. https://doi.org/10.1038/ngeo2962
Watanabe, M., Tatebe, H., 2019. Reconciling roles of sulphate aerosol forcing and internal variability in Atlantic multidecadal climate changes. Clim. Dyn. https://doi.org/10.1007/s00382-019-04811-3
Weisheimer, A., Schaller, N., O'Reilly, C., MacLeod, D.A., Palmer, T., 2017. Atmospheric seasonal forecasts of the twentieth century: multi-decadal variability in predictive skill of the winter North Atlantic Oscillation (NAO) and their potential value for extreme event attribution. Q. J. R. Meteorol. Soc. 143, 917–926. https://doi.org/10.1002/qj.2976
Wilcox, L.J., Highwood, E.J., Booth, B.B.B., Carslaw, K.S., 2015. Quantifying sources of inter-model diversity in the cloud albedo effect. Geophys. Res. Lett. 42, 1568–1575. https://doi.org/10.1002/2015GL063301
Wilcox, L.J., Highwood, E.J., Dunstone, N.J., 2013. The influence of anthropogenic aerosol on multi-decadal variations of historical global climate. Environ. Res. Lett. 8, 024033. https://doi.org/10.1088/1748-9326/8/2/024033
Wild, M., Ohmura, A., Makowski, K., 2007. Impact of global dimming and brightening on global warming. Geophys. Res. Lett. 34. https://doi.org/10.1029/2006GL028031
Wittenberg, A.T., 2009. Are historical records sufficient to constrain ENSO simulations? Geophys. Res. Lett. 36. https://doi.org/10.1029/2009GL038710
Wood, K.R., Overland, J.E., 2010. Early 20th century Arctic warming in retrospect. Int. J. Climatol. 30, 1269–1279. https://doi.org/10.1002/joc.1973
Woollings, T., Lockwood, M., Masato, G., Bell, C., Gray, L., 2010. Enhanced signature of solar variability in Eurasian winter climate. Geophys. Res. Lett. 37. https://doi.org/10.1029/2010GL044601
Yan, X.-H., Boyer, T., Trenberth, K., Karl, T.R., Xie, S.-P., Nieves, V., Tung, K.-K., Roemmich, D., 2016. The global warming hiatus: Slowdown or redistribution? Earths Future 4, 2016EF000417. https://doi.org/10.1002/2016EF000417
Zelinka, M.D., Andrews, T., Forster, P.M., Taylor, K.E., 2014. Quantifying components of aerosol-

cloud-radiation interactions in climate models. J. Geophys. Res. Atmospheres 119, 7599–7615. https://doi.org/10.1002/2014JD021710

Zhang, R., Delworth, T.L., Sutton, R., Hodson, D.L.R., Dixon, K.W., Held, I.M., Kushnir, Y., Marshall, J., Ming, Y., Msadek, R., Robson, J., Rosati, A.J., Ting, M., Vecchi, G.A., 2013. Have Aerosols Caused the Observed Atlantic Multidecadal Variability? J. Atmospheric Sci. 70, 1135–1144. https://doi.org/10.1175/JAS-D-12-0331.1

Zhang, X., Wan, H., Zwiers, F.W., Hegerl, G.C., Min, S.-K., 2013. Attributing intensification of precipitation extremes to human influence. Geophys. Res. Lett. 40, 5252–5257. https://doi.org/10.1002/grl.51010

Zhang, X., Zwiers, F.W., Hegerl, G.C., Lambert, F.H., Gillett, N.P., Solomon, S., Stott, P.A., Nozawa, T., 2007. Detection of human influence on twentieth-century precipitation trends. NATURE 448, 461-U4. https://doi.org/10.1038/nature06025

Zhang, Y., Wallace, J.M., Battisti, D.S., 1997. ENSO-like Interdecadal Variability: 1900–93. J. Clim. 10, 1004–1020. https://doi.org/10.1175/1520-0442(1997)010<1004:ELIV>2.0.CO;2

Tables

Table 1: Example of detection and attribution results from the literature, starting from the last millennium (top) to instrumentally based (bottom; note model simulations will not be identical, so scaling factors are indicative only). A detectable response in greenhouse gases is indicated by Y (at either the 5 or 10% significance level), and 'consistent' refers to a scaling factor encompassing '1', i.e. the model not needing to be rescaled to match observations. For analyses which have analysed individual models separately we give the fraction of models in which the forcing is detectable.

paper	Period/exp	models	Detection of greenhouse gas influence	Detection of other forcings
PAGES 2k Consortium et al. (2013); PAGES 2k-PMIP3 group (2015)	864-1840 1013-1989 1350-1840 recons.	PMIP3	Not attempted	All forcings detectable in NH continents but not SH
Schurer et al. (2013)	1400-1900, NH; reconstructions	PMIP	Y (most reconstructions, consistent)	Nat generally detectable and consistent, best guess <1.
Schurer et al. (2014)	1450-1900 NH multi-reconst.	HadCM3	Y	Volc detectable, solar consistent but not significant

Hegerl et al. (2011)	1500-1996, Europe only; proxy + instrumental	3 Last Millennium simulations	ANT ~ det. in winter and spring	volc. Detectable in EPOCH analysis, solar not robustly detectable
Schurer et al. (2018)	1862-2012 instrumental	CMIP5 individual models	Y (consistent)	OANT close to detection; NAT detectable, ~0.7 but consistent
Jones et al. (2013)	1901-2010 1906-2005 instrumental	CMIP5 individual models	Y 8/16 cases Y 8/15 and MM mean	Nat detectable 8/16 Nat detectable 8/15 and MM mean ; both: OANT mostly not detectable in indiidual .models
Jones and Kennedy (2017)	1906-2005 instrumental with uncertainty	CMIP5 MM	Y small uncertainty	All others combined D
Gillett et al. (2013)	1861-2010	CMIP5 and individual models	Y 7/9 and MM mean including model uncertainty	Nat detectable in 7/9 and MMM with model uncertainty OANT detectable in 5/9 cases and MMM only when not including model uncertainty
Ribes and Terray (2013)	1901-2010	CMIP5 and individual models	Y 4/10	Nat detectable in 4/10 and OANT detectable in 1/10 cases

Figures

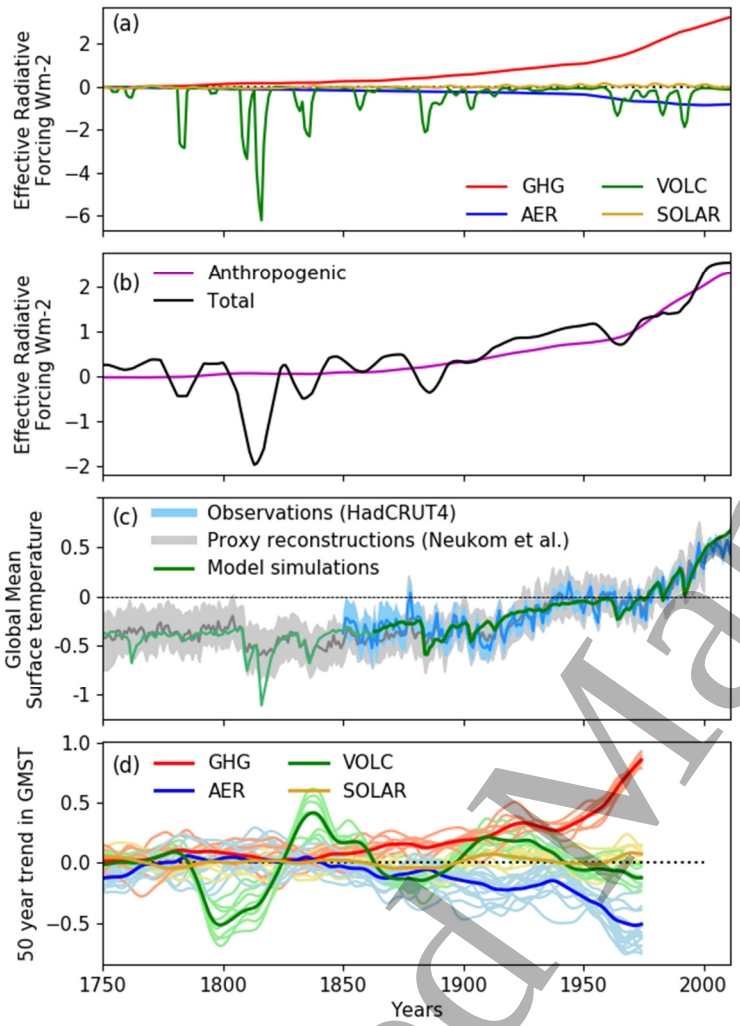

Figure 1: External forcing compared to observed global temperature data. a): Radiative forcing over the industrial period from IPCC AR5 (Myhre et al., 2013) for individual forcings (smoothed by a 3-year running mean), and b) decadally smoothed (11-year running mean, followed by a 7-year running mean; natural forcings centred on long-term average, 1750-2011) anthropogenic and combined forcing over the industrial period. c) observed (Morice et al., 2012) and reconstructed global temperature anomalies ([K], Neukom et al., 2019), as well as multi-model mean simulations which are generated by merging 23 last millennium simulations from 7 models: bcc-csm1-1(x1), CCSM4(x1), CESM1(x10), CSIRO-Mk3l(x3), GISS-E2-R(x3), HadCM3(x4), MPI-ESM-P(x1) with 109 CMIP5 historical simulations from 41 models (see methods), calculated from a 1961-1990 climatology. d) running 50-year trends (trend calculated from timeseries smoothed by a 5 then 3-year running average, plotted against central time point, [K/50 yrs]) that illustrate trends caused by individual forcings in two models (HadCM3 and CESM1) (thicker lines: multi-model mean, thinner lines: individual simulations).

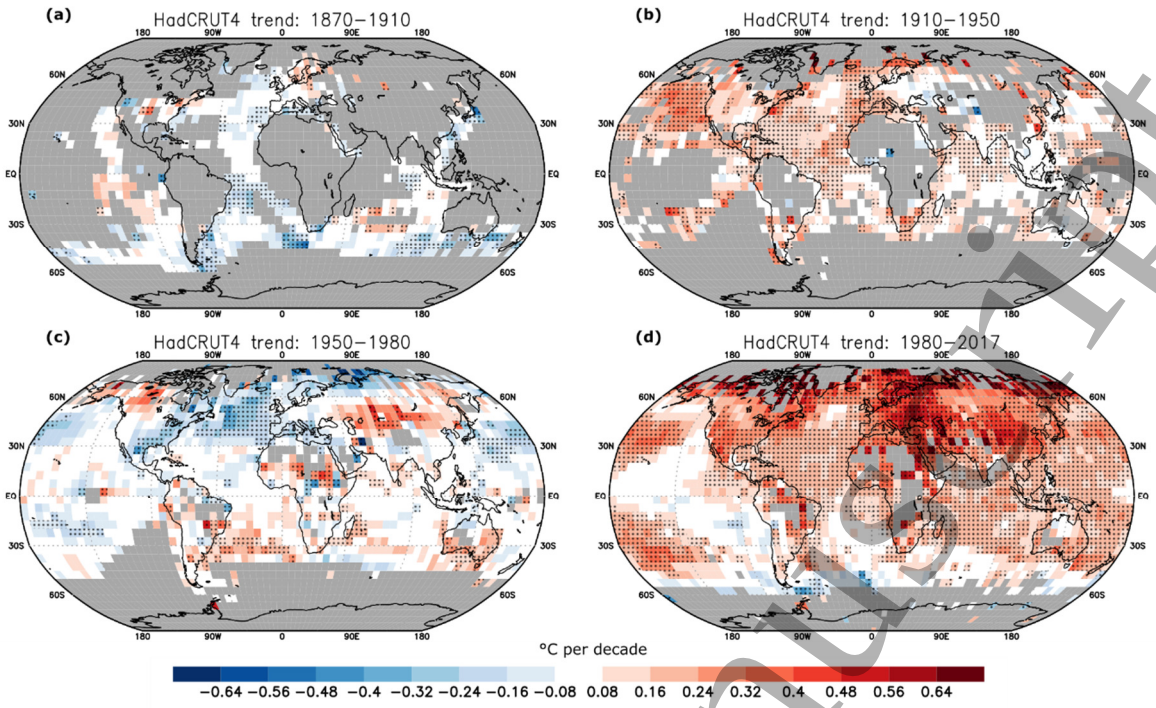

Figure 2. Long-term multi-year trends over the instrumental period. HadCRUT4 (Morice et al., 2012) 3-year running mean annual mean (November–October) trends over: (a) 1870–1910, (b) 1910–1950, (c) 1950–1980, and (d) 1980–2017. The 3-year annual means are constructed from averaging November–April and May–October anomalies, each smoothed with a 3-year running mean. Grey areas indicate regions where each overlapping 3-year segment does not contain at least one datapoint from both November–April and May–October. The slopes are stippled where significant at $p<0.05$ using a 2-tailed t-test, adjusted for autocorrelation induced by the 3-year running mean by increasing the regression standard error by a factor of $\sqrt{3}$, and by using 1 degree of freedom for every 3 years of length.

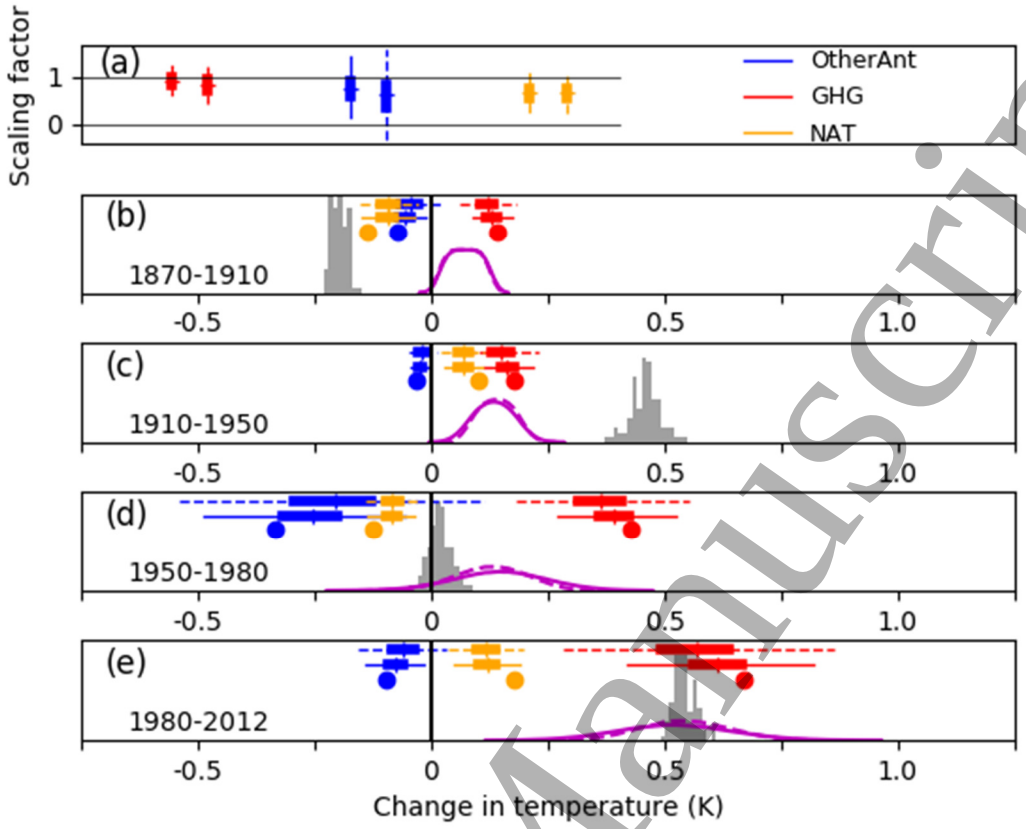

Figure 3: Estimated contribution by forcing to observed changes across the instrumental record. This is based on HadCRUT4 surface temperature data with histograms reflecting uncertainty (Morice et al., 2012). a) estimated magnitude of the response to forcing by greenhouse gases (GHG, red), other anthropogenic forcing (OtherAnt, blue) and natural forcing (solar and volcanic, NAT, yellow). Results are based on a Bayesian approach over the full period (1863-2012) using the multimodel mean response (Schurer et al., 2018); using global mean and hemispheric difference as spatial components, and decadally averaged timeseries). Values in the bottom four panels are calculated by scaling the linear trend by the best fit of the model fingerprint to observations over the entire record. The purple line is the combined anthropogenic contribution to the change in that period, the grey histogram is the range of observational values. The thick line indicates the 33-66th percentile, the thin line 5-95% of the uncertainty, and the continuous line is an estimate using prior information that favours scaling near one and avoids unphysical negative scaling, while the dashed line shows results for a flat prior between -1 and 3. Circles in each of the bottom panels indicate the multi-model mean estimate of the forced contribution without scaling. Note that the prior information makes little difference to the estimate of the total anthropogenic contribution, but does affect the estimate of individual forcings.

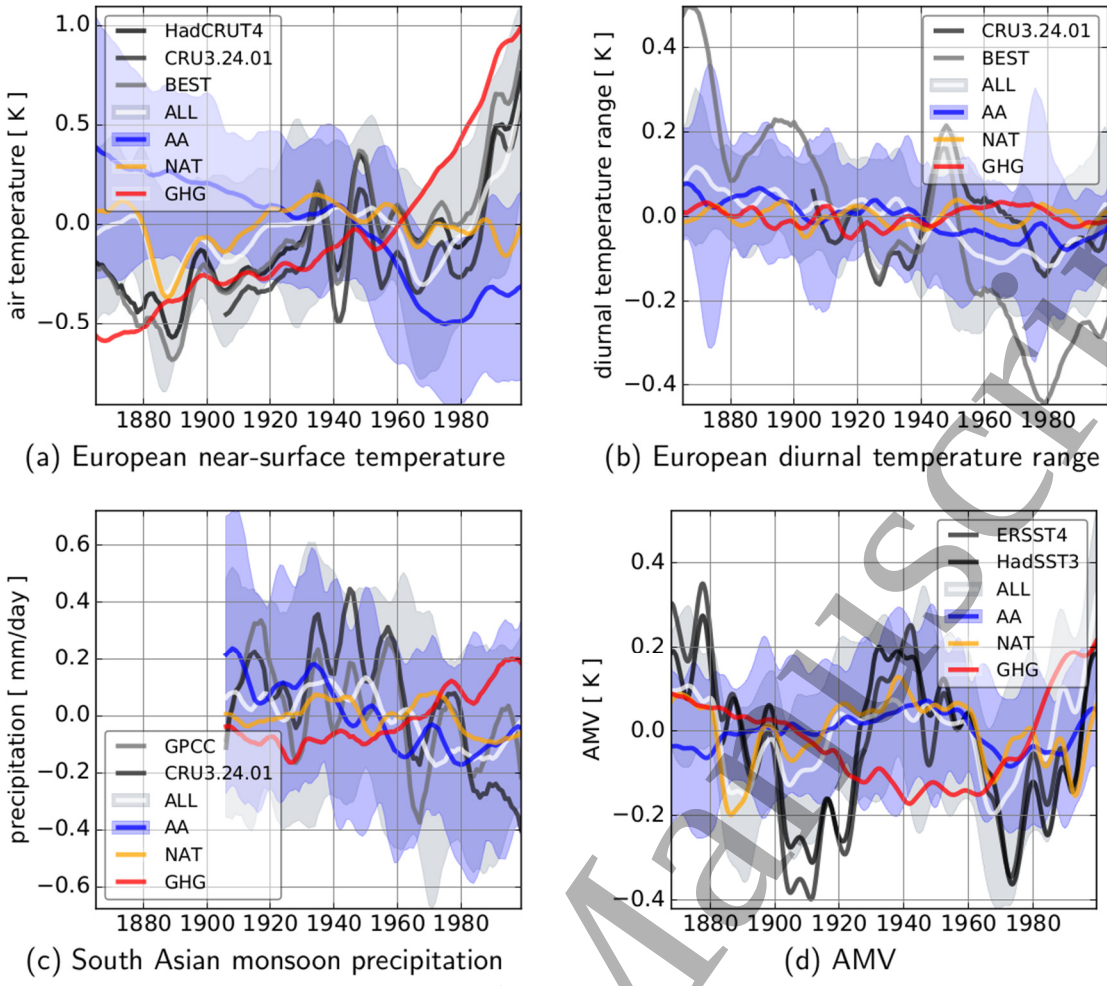

Figure 4 Aerosol influences on European climate, South Asian monsoon and Atlantic Multidecadal Variability. Anomalies of (a,b) annual-mean (a) near-surface temperature and (b) diurnal temperature range (a,b) over Europe (35-65°N,15°W-30°E, land only, area-weighted) similar to Undorf et al. (2018b), (c) summer (JJAS)-mean monsoon precipitation over South Asia (area definition as in Undorf et al., 2018c), and (d) the annual Atlantic Multidecadal Variability (AMV) index for (black, grays) observations and simulations with (red) greenhouse gas (GHG) forcing, (blue) anthropogenic aerosol (AA), and (yellow) natural (NAT) forcing only, and (white) all forcings together (ALL). Shown are the ensemble means (lines) and the 1.66σ range (shading) of each multi-model ensemble, smoothed by applying (a-c) 7- and 5-point and (d) 11- and 7-point filters consecutively. The shadings for GHG and NAT are omitted for clarity. (d) Sea surface temperatures (SSTs) are not available for all models, so surface temperatures over sea areas are used instead and compared with SST observations. The AMV is derived as in Undorf et al. (2018a). The models and the respective number of ensemble members used are CanESM2 [x5], CESM1-CAM5 [x1], CSIRO-Mk-3-6-0 [x5], GFDL-CM3 [x3], GISS-E2-R [x5], HadGEM2-ES [x4] (only in a and c), IPSL-CM5A-LR [x1], and NorESM1-M [x1].

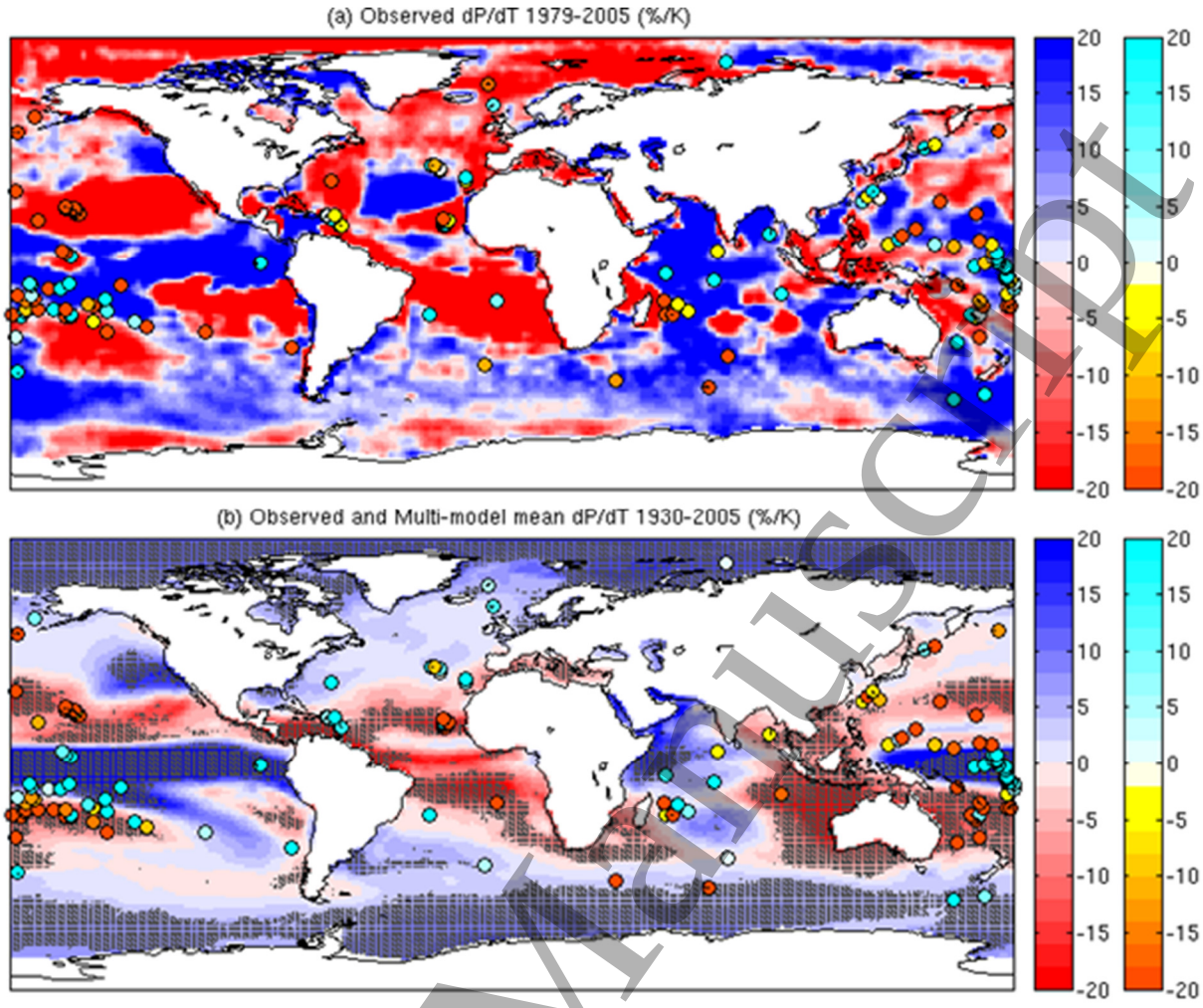

Figure 5 Spatial pattern of precipitation sensitivity (change in precipitation per degree of global mean warming, dP/dT) from satellite/gauge data. (a) Precipitation from the Global Precipitation Climatology Project (GPCP; Huffman et al., 2009; from 1979-2005) and (b) from multimodel historical simulations 1930-2005 compared to those from long island stations (dots; from CRUTS3.22; Harris et al., 2014 in both panels; only small islands used). Figure taken from Polson et al., 2016. 65% of gridboxes on top agree on the sign of dP/dT between satellite data and island stations, while 71% of gridboxes agree on the sign of dP/dT between the average dP/dT of individual historical simulations from CMIP5 and island stations. Hatching shows where 75% of CMIP5 simulations agree on the sign of dP/dT.

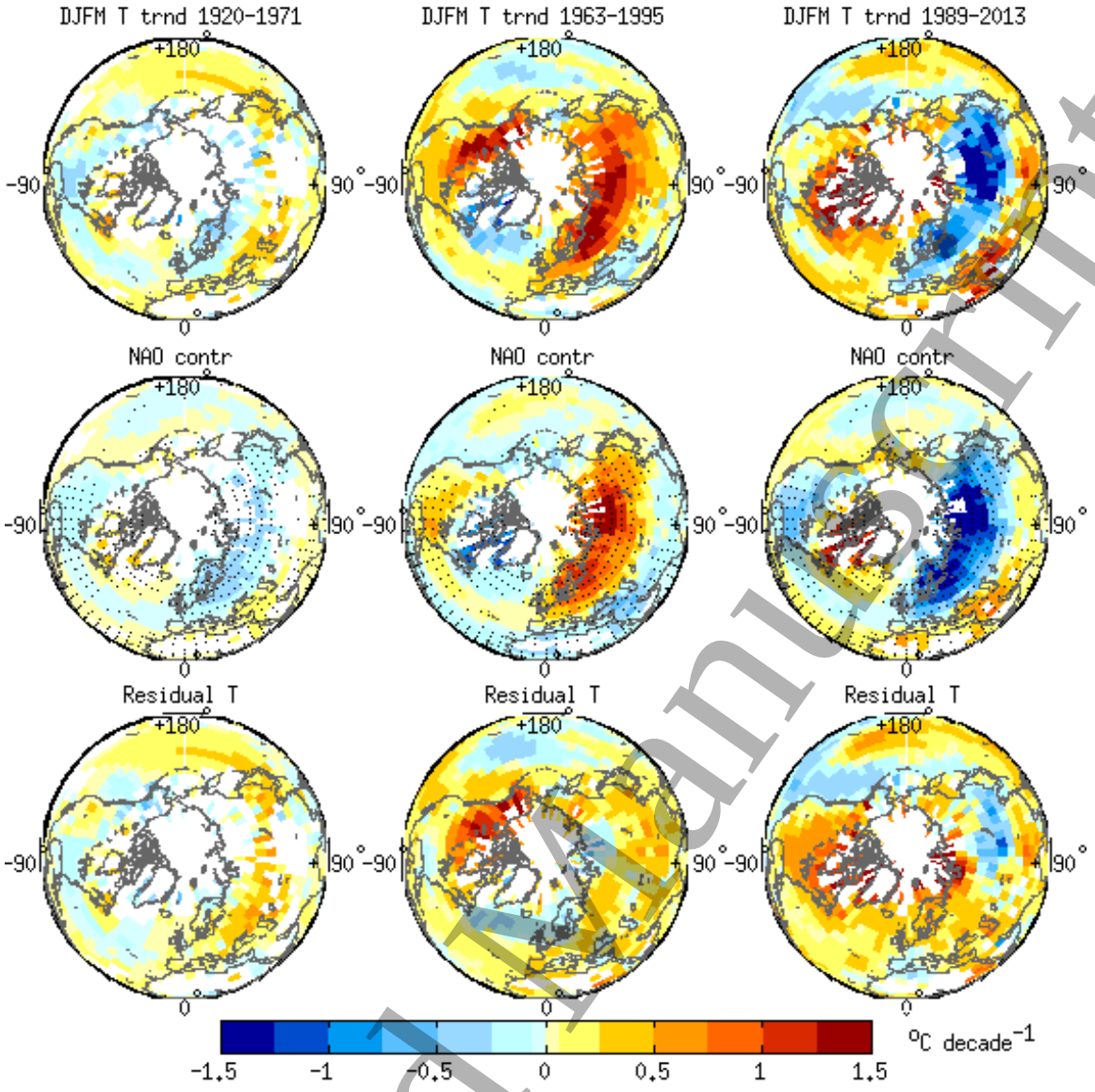

Figure 6: **Influence of North Atlantic Oscillation (NAO) variability on Northern Hemisphere winter temperature trends**. From Iles and Hegerl, 2017. Top row shows raw observed trend patterns [°C/decade], middle row estimated contribution by the NAO from interannual regression analysis (stippling indicates grid cells with a significant ($p < 0.05$) interannual relationship between the NAO and temperature), bottom row: trend pattern after linearly removing the contribution by the NAO; note that the residual results for the three periods are far more similar to each other and to the expected pattern in response to anthropogenic forcing than they were initially. Note that oceanic responses to trends in the NAO may enhance the long-term response over the North Atlantic and Arctic ocean basins.

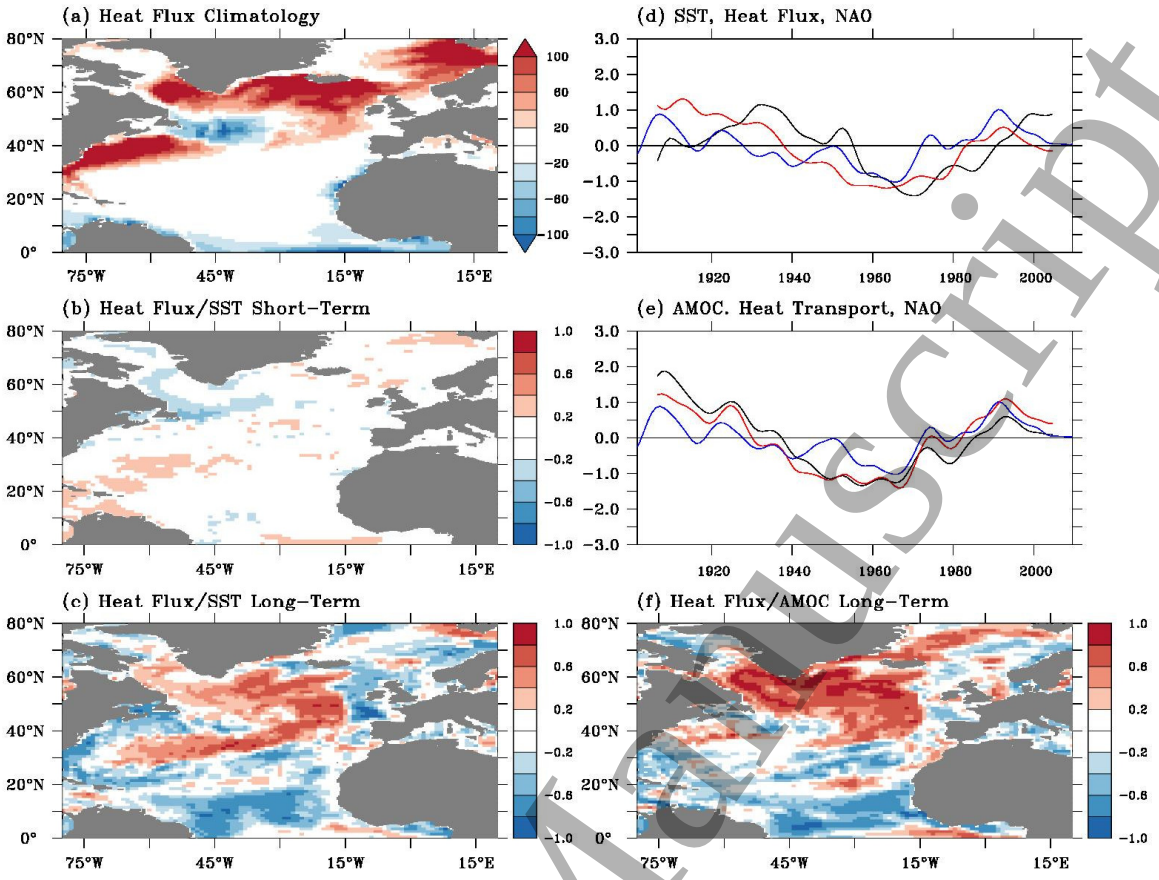

Figure 7: Relationship between the North Atlantic Oscillation and multidecadal ocean variations over 1901-2015. Multi-decadal variations in North Atlantic climate illustrated by the Max-Planck Institute ocean model (MPIOM) (Jungclaus et al., 2013) forced with century-long reanalysis ERA20C (Poli et al., 2016) (see text; figure adapted after Müller et al., 2015). Shown are (a) yearly mean surface heat flux climatology (sensible + latent, W/m^2), and correlation of averaged yearly mean SST (80°W-0°, 35°-50°N) with surface heat flux for (b) short-term variations (1-10yr; high-pass filtered) and (c) long-term variations (>10yr; low-pass filtered). Positive values indicate heat release into atmosphere. (d) standardized time series of 10-yearly mean SST (black, 80°W-0°, 35°-50°N), surface heat flux (red, 80°W-0°, 40°-60°N), and winter (JFM) NAO index based on Hurrell station index (blue). SST and surface heat fluxes are taken from the MPIOM. (e) 10-year running mean of AMOC (black, 26°N and 1000 m depth), integrated northern heat transport (red, 26°N) and the JFM NAO index (blue). All time series are standardized. (f) Correlations of yearly mean AMOC 26°N with surface heat flux for long-term variations (>10yr).

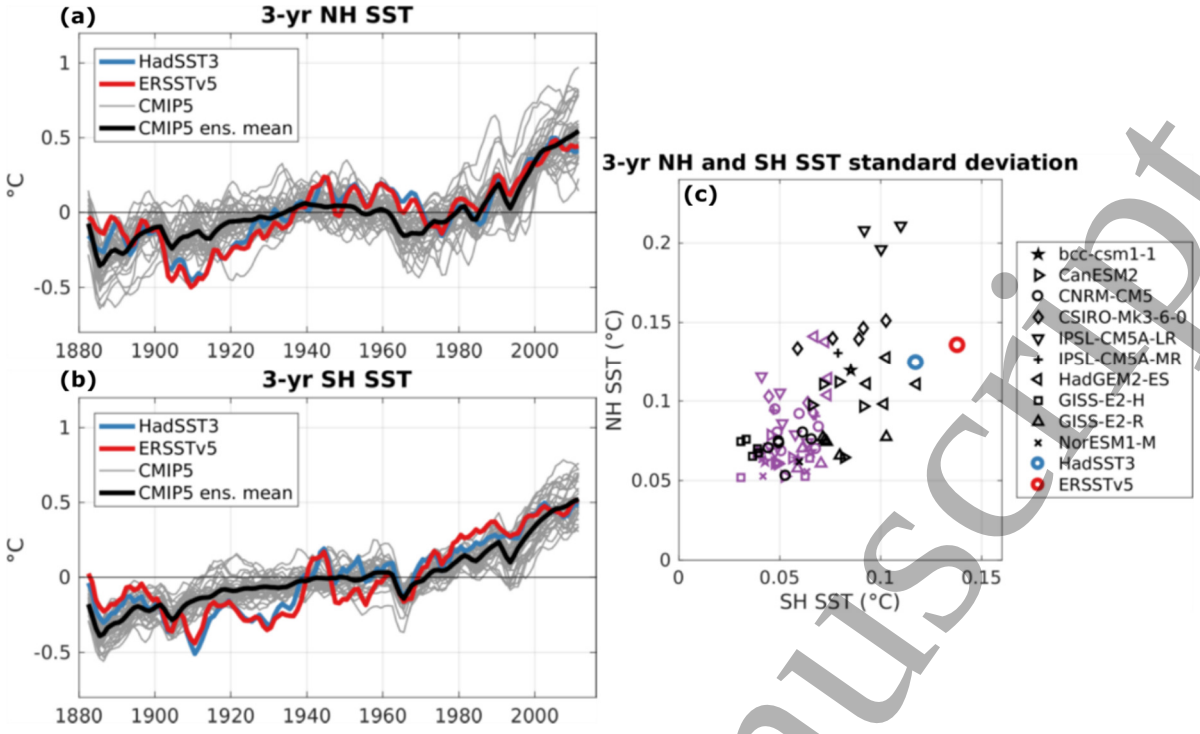

Figure 8: Consistency between simulated and observed changes in hemispheric-wide SST. a) Northern hemisphere (NH) and (b) Southern Hemisphere (SH) running 3-year annual mean (December–November) time series of SST anomalies from 1881-2012 for HadSST3 (Kennedy et al., 2011a, 2011b) and ERSSTv5 (Huang et al., 2017) observations and CMIP5 historical simulations. CMIP5 results are based on 36 realizations from 10 models and masked to HadSST3's early-20th century coverage (Friedman et al., in review). Thin lines show individual realizations; the solid black line shows the multi-model ensemble mean. (c) Comparison of NH and SH 3-year SST standard deviations. The CMIP5 historical ensemble mean is subtracted from the observations and the historical realizations, shown in black. Purple markers show standard deviations of 132-year pre-industrial control segments from the 10 CMIP5 models.

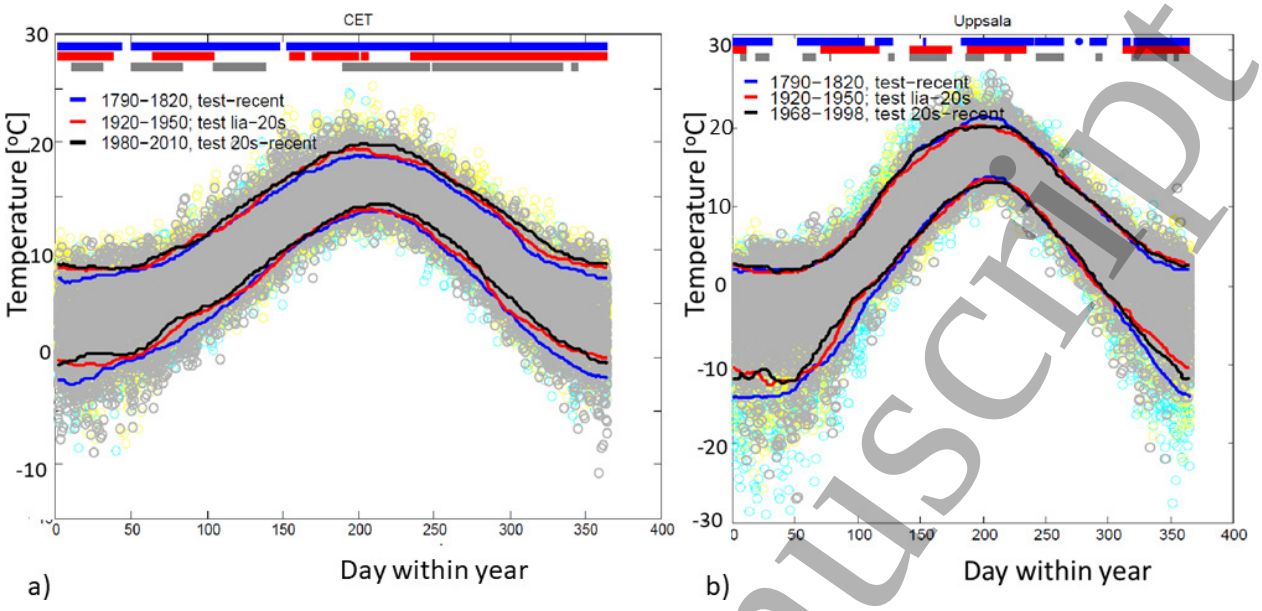

Figure 9: **Long-term change in daily temperature variability**. Daily temperatures (°C) plotted against [day/year] from a) the Central England time series (Parker et al., 1992) and b) Uppsala, Sweden (see text; Moberg et al., 2002). Dots are individual years, and lines represent the 10th and 90th percentiles based on smoothed (11-day averaged) daily climatology. Bars on top illustrate where three periods considered show significantly different daily temperature distributions (based on a Mann Whitney U test): the early 19th century (1790-1820, blue; with daily data cyan; blue bar on top where different from recent, red where different from early 20th century), the early 20th century (1920-1950, red, daily data yellow; grey bar on top where significantly different from recent) and the recent period (1980-2010, black, daily data grey). Note significant changes across much of the seasonal cycle between all periods with strong change in winter extremes.